



HHS Public Access

Author manuscript

J Med Chem. Author manuscript; available in PMC 2023 November 24.

Published in final edited form as:

J Med Chem. 2022 November 24; 65(22): 15238–15262. doi:10.1021/acs.jmedchem.2c01170.

Structure–Activity Studies of 1*H*-Imidazo[4,5-*c*]quinolin-4-amine Derivatives as A₃ Adenosine Receptor Positive Allosteric Modulators

Lucas B. Fallot⁺,

Molecular Recognition Section, Laboratory of Bioorganic Chemistry, National Institute of Diabetes and Digestive and Kidney Diseases, National Institutes of Health, Bethesda, Maryland 20892, United States

Department of Biochemistry and Molecular Biology, Uniformed Services University of the Health Sciences, Bethesda, Maryland 20814, United States

Department of Chemistry and Life Science, United States Military Academy, West Point, New York 10996, United States

R. Rama Suresh⁺,

Molecular Recognition Section, Laboratory of Bioorganic Chemistry, National Institute of Diabetes and Digestive and Kidney Diseases, National Institutes of Health, Bethesda, Maryland 20892, United States

Courtney L. Fisher,

Department of Pharmacology and Toxicology, Medical College of Wisconsin, Milwaukee, Wisconsin 53226, United States

Veronica Salmaso,

Molecular Recognition Section, Laboratory of Bioorganic Chemistry, National Institute of Diabetes and Digestive and Kidney Diseases, National Institutes of Health, Bethesda, Maryland 20892, United States

Robert D. O'Connor,

Molecular Recognition Section, Laboratory of Bioorganic Chemistry, National Institute of Diabetes and Digestive and Kidney Diseases, National Institutes of Health, Bethesda, Maryland 20892, United States

Corresponding Author Kenneth A. Jacobson – Molecular Recognition Section, Laboratory of Bioorganic Chemistry, National Institute of Diabetes and Digestive and Kidney Diseases, National Institutes of Health, Bethesda, Maryland 20892, United States, Phone: 301-496-9024; kennethj@niddk.nih.gov; Fax: 301-451-5364.

⁺ Author Contributions

L.B.F. and R.R.S. contributed equally.

The authors declare no competing financial interest.

ASSOCIATED CONTENT

Supporting Information

The Supporting Information is available free of charge at <https://pubs.acs.org/doi/10.1021/acs.jmedchem.2c01170>.

Additional synthetic routes, spectral and HPLC data, off-target binding inhibition data, pharmacological data, ADMET procedures, and data for compounds **18** and **39**, including Schemes S1–S6, Tables S1–S8, and Figures S1–S5 (PDF)

Molecular formula strings file (CSV)

Heavy atoms coordinates of the predicted poses of compounds **7** and **17** at the orthosteric binding site (ZIP)

Complete contact information is available at: <https://pubs.acs.org/10.1021/acs.jmedchem.2c01170>

Noy Kaufman,

Molecular Recognition Section, Laboratory of Bioorganic Chemistry, National Institute of Diabetes and Digestive and Kidney Diseases, National Institutes of Health, Bethesda, Maryland 20892, United States

Zhan-Guo Gao,

Molecular Recognition Section, Laboratory of Bioorganic Chemistry, National Institute of Diabetes and Digestive and Kidney Diseases, National Institutes of Health, Bethesda, Maryland 20892, United States

John A. Auchampach,

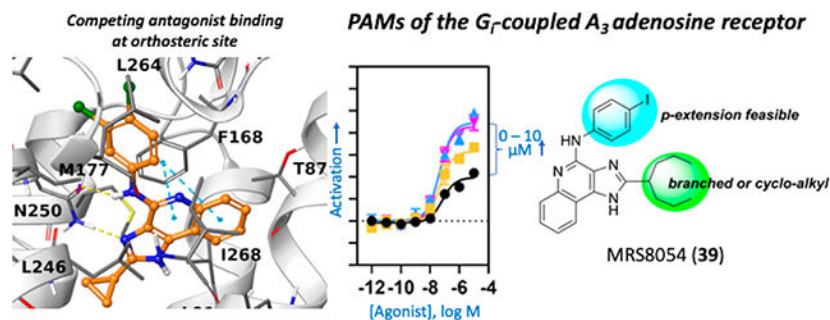
Department of Pharmacology and Toxicology and Cardiovascular Center, Medical College of Wisconsin, Milwaukee, Wisconsin 53226, United States

Kenneth A. Jacobson

Molecular Recognition Section, Laboratory of Bioorganic Chemistry, National Institute of Diabetes and Digestive and Kidney Diseases, National Institutes of Health, Bethesda, Maryland 20892, United States

Abstract

We previously reported 1*H*-imidazo[4,5-*c*]quinolin-4-amines as A₃ adenosine receptor (A₃AR) positive allosteric modulators (PAMs). A₃AR agonists, but not PAMs, are in clinical trials for inflammatory diseases and liver conditions. We synthesized new analogues to distinguish 2-cyclopropyl antagonist **17** (orthosteric interaction demonstrated by binding and predicted computationally) from PAMs (derivatives with large 2-alkyl/cycloalkyl/bicycloalkyl groups). We predicted PAM binding at a hydrophobic site on the A₃AR cytosolic interface. Although having low Caco-2 permeability and high plasma protein binding, hydrophobic 2-cyclohept-4-enyl-*N*-3,4-dichlorophenyl, MRS7788 **18**, and 2-heptan-4-yl-*N*-4-iodophenyl, MRS8054 **39**, derivatives were orally bioavailable in rat. 2-Heptan-4-yl-*N*-3,4-dichlorophenyl **14** and 2-cyclononyl-*N*-3,4-dichlorophenyl **20** derivatives and **39** greatly enhanced CI-IB-MECA-stimulated [³⁵S]GTPγS binding *E*_{max}, with only **12b** trending toward decreasing the agonist EC₅₀. A feasible route for radio-iodination at the *p*-position of a 4-phenylamino substituent suggests a potential radioligand for allosteric site binding. Herein, we advanced an allosteric approach to developing A₃AR-activating drugs that are potentially event- and site-specific in action.

Graphical Abstract

INTRODUCTION

Agonists of the four subtypes of adenosine receptors (ARs) are an appealing ligand class for drug development due to the many salutary actions of adenosine, such as tissue repair and protection against ischemia and other organ stress.¹ Activation of the G_i-coupled A₃AR subtype is associated with attenuating chronic neuropathic pain, heart and brain ischemic preconditioning, and anti-inflammatory effects, without causing cardiovascular side effects.^{2,3} The A₃AR is overexpressed in immune and cancer cells, adding to its potential as a possible therapeutic target.³ At present, A₃AR agonists are in Phase 2/3 clinical trials for psoriasis, due to their anti-inflammatory properties, and liver diseases, i.e., hepatocellular carcinoma and non-alcoholic steatohepatitis (NASH).⁴

Allosteric modulators bind to sites that are topographically distinct from the orthosteric binding site for native agonists and can exert their effects through receptor conformation changes beyond those induced by orthosteric ligands.⁵ Various types of allosteric modulators differ in their pharmacological effects. Positive allosteric modulators (PAMs) may improve agonist affinity, potency, and/or efficacy, while negative allosteric modulators (NAMs) do the opposite. Some allosteric modulators can induce a characteristic functional response in the absence of an agonist, i.e., ago-PAMs.⁶

The hallmark advantage of PAMs over orthosteric agonists is that they can be event- and site-specific in action.⁷ Because adenosine is endogenously elevated in response to localized distress signals within the body, a pure PAM will enhance the protective function of adenosine only when and where it is elevated, thereby reducing the risk of side effects.⁸ A second advantage of developing AR PAMs over orthosteric ligands is the possibility of achieving a high selectivity for a single AR subtype, since PAMs typically bind to regions that are more variable between receptor subtypes. Third, AR agonists have multiple potential pharmaceutical applications in the central nervous system (CNS),⁹ but current A₃AR orthosteric agonists, mainly nucleosides, tend to have low blood–brain barrier (BBB) permeability, with typically only a few percent or less available in the CNS.^{10–13} Therefore, BBB-penetrating PAMs might be preferable over AR nucleoside agonists for CNS applications. Lastly, it might be possible to develop biased PAMs that selectively enhance certain A₃AR-induced signaling pathways.^{14,15}

At least four heterocyclic classes have been reported to act as A₃AR allosteric modulators (Chart 1): amilorides,¹⁶ represented by 5-(*N,N*-hexamethylene)amiloride (HMA, **1**); PAMs shown are **2** (3-(2-pyridinyl) isoquinolines;¹⁷ 2,4-disubstituted quinolines, represented by **3**; and, 1*H*-imidazo[4,5-*c*]quinolin-4-amines (**4–12**),^{18–20} including *N*-(3,4-dichloro-phenyl)-2-cyclohexyl-1*H*-imidazo[4,5-*c*]quinolin-4-amine (**7**, LUF6000).²¹

We previously explored the structure–activity relationship (SAR) of the 1*H*-imidazo[4,5-*c*]quinolin-4-amine family of A₃AR PAMs.^{19,20,22} Prototypical A₃AR PAM **7**, which is now being considered for clinical testing for erectile dysfunction,²³ slowed A₃AR agonist dissociation.^{19,20} It enhanced maximal efficacy (E_{\max}) at the human (h) A₃AR (but not the mouse homologue)²⁴ without influencing agonist potency, possibly due to simultaneous competitive interactions at the orthosteric binding site.^{17,18} The A₃AR PAM activity of

imidazoquinolinamine derivatives is often accompanied by variable degrees of apparent receptor antagonist activity.^{19,20} Based on findings with chimeric receptors composed of an A₃AR from a responding (human) and a non-responding (mouse) species, we predict that PAM activity results from binding to an allosteric site located within inner/cytosolic A₃AR regions, exclusive of the orthosteric binding site.²⁴ The chimeric receptors indicated that a 2-cyclopropyl derivative interacts primarily with the orthosteric site as a competitive antagonist, and the corresponding 2-cyclohexyl derivative **7** can interact with both sites. The possibility that **7** might negatively modulate A₃AR agonists by binding to the same intracellular allosteric site, i.e., NAM activity, has been ruled out.²⁴

In this study, we have extended the recent expansion and contraction of the 2-cyclohexyl ring of **7** by Fisher et al.²⁴ with additional 1*H*-imidazo[4,5-*c*]quinoline-4-amine derivatives as hA₃AR PAMs through modifications at the 4-arylamino and/or the 2 position of the imidazoquinoline scaffold. We functionalized the rings with polar groups to try to reduce lipophilicity and improve aqueous solubility, as well as introduced bridging groups to determine if there is an A₃AR-preferred conformation of 2 position substituent. We also explored the effect of various 4-arylamino substitutions on positive allosteric enhancement. Here we describe the synthetic methods for the newly prepared analogues, including those reported by Fisher et al.²⁴

The objectives of this study were: to expand the SAR of 1*H*-imidazo[4,5-*c*]quinolin-4-amine derivatives related to **7** to identify high efficacy A₃AR PAMs, including those bearing hydrophilic and conformationally constrained groups; to devise a shorter synthetic route to derivatize 1*H*-imidazo[4,5-*c*]quinolin-4-amines than the ones previously reported;^{18–20} and to obtain a baseline example of the absorption, distribution, metabolism, excretion, and toxicity (ADMET) properties of potential lead compounds from this series.

RESULTS AND DISCUSSION

Description of Synthetic Compound List.

Four groups of 1*H*-imidazo[4,5-*c*]quinolin-4-amine derivatives were synthesized for A₃AR pharmacological characterization, as listed in Table 1 (**5–8**, **13–39**), including six compounds reported earlier (**5–8** and **12**).¹⁹ The final step reaction yields are shown in Table S1. The first group of derivatives (**5–8**, **13–23**) has hydrophobic alkyl and cycloalkyl substitutions at the 2 position of the 1*H*-imidazo[4,5-*c*]quinolin-4-amine scaffold with the 3,4-dichlorophenyl group at the 4-amino position, which was shown in previous SAR studies to improve A₃AR PAM activity and subtype selectivity.^{19,20} The second group of derivatives (**24–29**) includes bridged 2-bicyclic substitutions, based on the favorable PAM activity of compounds **8** and **19**, as well as the *exo*-norbornanyl and adamantan-1-yl derivatives **12a** and **12b** (Chart 1E). The third group (**30–34**) has hydrophilic oxygen-containing functionality introduced on a 2-cycloheptyl ring and a 3,4-dichlorophenyl group at the 4-amino position. Lastly, the fourth group (**35–39**) has a cyclohexyl ring or a heptan-4-yl moiety at the 2 position combined with various *p*-substituted 4-phenylamino groups. Prior studies showed tolerance of 4-methoxy and 4-chloro substitutions at the 4-phenylamino position (**10** and **11**, Chart 1D), resulting in promising A₃AR allosteric enhancement based on a slower dissociation rate and increased E_{\max} of agonists.¹⁹ Compounds **29**

and **32–34** were racemic mixtures. For most of the analogues, we incorporated the 4-(3,4-dichlorophenylamino) substitution based on previous studies in which this group, compared to other haloaryl groups (3,5- and 2,4-dichloroaniline derivatives), had favorable PAM activity as indicated by effects on agonist dissociation kinetics and efficacy.²⁰

Chemical Synthesis.

3,4-Diaminoquinoline intermediate **53** and final compounds **13**, **14**, and **16** were prepared by literature procedures (Scheme S1).¹⁹ A shorter synthesis than the previously reported 9-step route,¹⁹ requiring only 6 steps, was developed to create a new series of 1*H*-imidazo[4,5-*c*]quinolin-4-amine derivatives (Scheme 1). The first four steps closely followed a reported synthetic route used to synthesize a non-adenosine-related series of 2-(*p*-substituted-phenyl)-4-phenyl-1*H*-imidazo[4,5-*c*]quinoline derivatives, which differ from the present compounds in having a 4-phenyl instead of a 4-aminophenyl substitution.²⁵

In the first step of the 6-step route (Scheme 1), quinoline-2,4-diol **40** was nitrated with nitric acid to produce 3-nitroquinoline-2,4-diol **41**. **41** was then chlorinated with phenylphosphonic dichloride to afford 2,4-dichloro-3-nitroquinoline **42**. The step-2 product was then aminated in step-3 with 28% aq. ammonia to give regioselectively 2-chloro-3-nitroquinolin-4-amine **43**. Subsequently, in step-4 Fe powder and hydrochloric acid reduced the 3-nitro group to an amine to provide the vicinal diamine, 2-chloroquinoline-3,4-diamine **44**.²⁵

Two alternative step-5 protocols condensed the vicinal diamine with a carboxylic acid followed by cyclization. The first reaction protocol (see Scheme 1, general procedure A (v)), utilized polyphosphoric acid (PPA) for the condensation between 2-chloroquinoline-3,4-diamine and an appropriate carboxylic acid **45**, followed by cyclization to the imidazole **46**.¹⁹ The second reaction protocol (see general procedure B (vi)), required two steps without isolation of the intermediate. Initially, an acyl imidazolium adduct formed between the coupling agent tetramethylchloroformamidinium hexafluorophosphate (TCFH) and *N*-methylimidazole (NMI), which provided an electrophile to activate the appropriate carboxylic acid **45**.²⁶ The vicinal diamine **44** was acylated to produce an amide intermediate (not shown). A similar published vicinal diamine reaction uses room temperature,²⁶ but we found that heating at 60 °C brought the reaction to completion, increasing the yield. The crude amide was subjected to a subsequent base-catalyzed cyclization reaction to form the imidazole ring in **46** and incorporate a 2 position substitution on the imidazoquinoline scaffold.

The last step, a C–N cross-coupling reaction, was performed using three different reaction protocols. The first protocol used the palladium catalyst tris(dibenzylideneacetone) dipalladium(0) (Pd₂(dba)₃) (general procedure C (viii) in Scheme 1),^{27–29} while the second used a water-activated palladium acetate (Pd(OAc)₂) catalyst (general procedure D (ix) in Scheme 1).²⁸ We attempted to improve the cross-coupling reaction yield using Pd(OAc)₂ rather than the Pd₂(dba)₃ catalyst, because the removal of the sizable dba (dibenzylideneacetone) ligand during the palladium catalyst activation might sterically hinder the oxidative addition of the aryl halide during the catalytic cycle.²⁷ However, higher

yields were obtained using the step-6 general procedure C than with the general procedure D. The third reaction protocol was a microwave-assisted reaction in ethanol at 130 °C to achieve the final 1*H*-imidazo[4,5-*c*]quinolin-4-amine derivative (general procedure E (x) in Scheme 1).¹⁹

Compounds **13–15** have 2-alkyl substitutions, with compound **15** included to investigate the effect of terminal hexafluoro substitution on the pharmacological activity of compound **14**.³⁰ The carboxylic acid precursor of compound **15** was prepared by a procedure reported in a patent (Scheme S2).^{31,32} Compound **16** introduced a trifluoromethyl group at the 4 position of the cyclohexyl ring of a reference PAM, **7**. Final compounds **13–22** were prepared with the step-6 general procedure C, having yields ranging from 5% to 51%. Compound **23** was synthesized using the step-6 general procedure E with the C–N cross-coupling of the 4-chloro in step-5 product to produce 3,4-dichloroaniline in 25% yield. Most carboxylic acids used for the construction of the cycloaliphatic rings in compounds **7** and **17–23** (starting from compounds **46e–o** using the synthetic procedures in Scheme 1) were commercially available, except for the cyclononane- and cyclodecanecarboxylic acids, which were synthesized from a Favorskii ring contraction of their respective α -bromo-cycloketones (Scheme S3).

Compounds **24–27** were produced using the step-6 general procedure D, having yields ranging from 2% to 33%. In the cyclopropanation reaction of alkene derivative **18** to form compound **28**,³³ only the *cis* stereoisomer was recovered (Scheme 1, the imidazole group is *trans* with respect to the cyclopropane), which was confirmed by 1D-NOE NMR.

Bicyclo[2.2.2]oct-2-ene derivative **29** was the only two-carbon bridged derivative with a double bond to provide extra rigidity to the ring system. The precursor bicyclic carboxylic acids were obtained upon saponification of the methyl ester products formed from a Diels–Alder reaction between 1,3-cyclohexadiene and methyl acrylate (Scheme S4).^{34,35} Two pairs of enantiomers that are diastereoisomers to one another were isolated from the Diels–Alder reaction, the majority being the *endo* enantiomeric pair, likely due to the lower transition state energy favoring the formation of the *endo* over *exo* stereoisomers. Thus, compound **29** is a racemic mixture of *endo* enantiomers, which was confirmed by 1D-NOE. The double bond of 2-cycloheptenyl derivative **18** allowed hydrophilic oxygen-containing functional groups to be installed (Scheme 1). Two diastereomeric oxirane compounds, **30** and **31**, were produced and resolved from the same epoxidation reaction of compound **18** using *m*-CPBA.³⁶ The distinguishing characteristic between these two diastereomers is the chemical shift of the ring proton (*CH*) on the carbon atom connected to the 2 position of the 1*H*-imidazo[4,5-*c*]quinolin-4-amine, which was δ 2.71 and δ 3.07 ppm for **30** and **31**, respectively, in the ¹H NMR spectrum. The structures of **27**, **29** and **30** were confirmed by 1D and 2D NMR (Supporting Information). Compounds **33** and **34** were made in the same hydroboration–oxidation reaction³⁷ and isolated as racemic mixtures, being enantiomeric pairs that are diastereomers to one another. The assignment of the configuration of compound **33** was similarly confirmed by 1D-NOE (Supporting Information). Compound **32** was made from treating a mixture of compounds **33** and **34** with the oxidizing agent Dess–Martin periodinane,³⁸ producing the racemic carbonyl enantiomers.

Compounds **35** and **36** have 4-iodophenyl and 4-bromophenyl substitutions, respectively. Both were produced using the step-6 general procedure E microwave-assisted reaction between a 4-chloro-2-cyclohexyl-imidazo[4,5-*c*]-quinolinamine **46**, the step-5 product, with the corresponding *p*-iodo- or *p*-bromo-aniline in ethanol (Scheme 1). Compound **37**, having a methyl acrylate 4 position substitution on the phenylamino moiety, was generated from a Heck reaction between compound **36** and methyl acrylate using a Pd(OAc)₂ catalyst (Scheme 1)³⁹ as the *E*-isomer. Compound **38** has a *p*-(5-chlorothiophen-2-yl)ethynyl substitution, and was prepared by a Sonogashira reaction between compound **35** and 2-chloro-5-ethynylthiophene using a bis(triphenylphosphine) palladium II dichloride catalyst (Scheme 1).^{40,41} A reaction using *p*-bromo derivative **36** was unsuccessful, but using *p*-iodo derivative **35** provided the desired product **38** (Scheme 1). Compound **39** was produced to study the effect of an I-label and to provide a potential allosteric radioligand. Two trialkylstannyl derivatives, **48** and **49**, were synthesized from compound **39** using a bistriphenylphosphine palladium dichloride catalyst with hexamethylditin or hexabutyliditin, respectively (Scheme S5).⁴² They are potential precursors for a radio-iodination reaction to produce a ¹²⁵I radioligand (Scheme S6).⁴³

Pharmacological Characterization.

Two assays using fixed PAM concentrations characterized the effects of the new derivatives on hA₃AR agonist radioligand ([¹²⁵I]N⁶-(4-amino-3-iodobenzyl)adenosine-5'-*N*-methyluronamide **50**, [¹²⁵I]I-AB-MECA) binding. Pharmacological results for a subset of these compounds (**5–8**, **14** and **17–23**) were reported by Fisher et al. and are included here for comparison.²⁴ This first assay (Figure 1) consisted of measuring the degree of radioligand dissociation after a standard time delay (3 h) following the addition of an excess of an unlabeled AR agonist (adenosine-5'-*N*-ethylcarboxamide **51**, NECA), reflecting the effect on dissociation rate (as a PAM would slow the dissociation). The second assay (Figure 2) consisted of measuring the influence of each modulator on the relative % binding of the radioligand at the hA₃AR after a long duration of incubation (18 h), at which point equilibrium conditions were achieved. A third assay, a functional assay, consisted of a [³⁵S]GTPγS binding assay to determine the potency of agonist (2-chloro-N⁶-(3-iodobenzyl)-5'-*N*-methylcarboxamidoadenosine **52**, CI-IB-MECA) as an EC₅₀ value (concentration of half-maximal activation) in hA₃AR activation and its *E*_{max} in the presence of the indicated compound. All three assays used membranes prepared from human embryonic kidney (HEK) 293 cells overexpressing the hA₃AR.

In Figure 1, single-point dissociation assays were conducted to measure the relative influence of each derivative on dissociation of **50** from the hA₃AR 60 min after initiation of dissociation by the addition of a competitive AR agonist **51** at a saturating concentration of 100 μM (Table S2). The horizontal dotted line represents the control amount of agonist radioligand that remained bound in the absence of a 1*H*-imidazo[4,5-*c*]quinolin-4-amine derivative, i.e., 26% of the amount bound at time 0. Thus, bars significantly above the line represent compounds that had a net effect to increase the amount of radioligand remaining bound, presumably by allosterically slowing the agonist dissociation rate, i.e., PAM activity.

Compounds **13–16** showed varying results, with 2-(heptan-4-yl) derivative **14** slowing agonist dissociation the most, with 71% of the radioligand remaining bound. Despite being the hexa-fluoro equivalent of compound **14**, compound **15** did not slow agonist dissociation compared to the control (P -value = 0.958).

Compounds **17** (cyclopropyl), **5** (cyclobutyl) through **8** (cycloheptyl), and **18** (cyclooctyl) through **23** (cyclododecyl) represent the 2-cycloalkyl-substituted analogues, ranging from 3 to 12 carbons. As the hydrophobic ring system increased from cyclopropyl **17** to cyclo-octyl **19**, there was a steady increase in percent radioligand remaining hA₃AR-bound compared to control. The following compounds displayed the greatest reduction in dissociation (P -values < 0.05, Student's t test), ranging from 45% to 54% left remaining: 2-cyclohexyl **7**, 2-cycloheptyl **8**, 2-cyclohept-4-enyl **18**, and 2-cyclooctyl **19**. With larger rings, radioligand dissociation was not significantly slowed compared to control (P -values = 0.188, 0.786, 0.808, and 0.735, for cyclononyl **20** to cyclododecyl **23**, respectively).

exo-Norbornanyl **12a**, adamantan-1-yl **12b**, and **24–29** represent bi- and tricyclic ring systems of varying sizes. Except for compounds **12a** and **29**, all compounds slowed the agonist dissociation compared to the control. The percent of radioligand remaining bound in the presence of modulators **12b** and **24–28** ranged from 45% to 52%. The compounds with hydrophilic substitutions on the 2-cycloheptyl ring, **30–34**, showed no net slowing of radioligand dissociation compared to the control.

Among the p -substituted 4-phenylamino derivatives **35–38**, compounds **35** (4-iodophenyl) and **36** (4-bromophenyl) slowed the radioligand dissociation rate the most, with 57% and 56% radioligand remaining, respectively. However, compounds **37** ((*E*)-methyl-3-(4-aminophenyl acrylate) and **38** (5-chlorothiophen-2-yl)ethynyl)phenyl) did not significantly slow the agonist dissociation rate compared to the control (P -values = 0.052 and 0.450, respectively). Compound **39**, with combined features of compounds **14** and **35**, i.e., 2-(heptan-4-yl) and 4-iodophenylamino substitutions, considerably slowed radioligand dissociation with 65% remaining A₃AR-bound.

Figure 2 shows single-point equilibrium binding assay results: the positive, negative, or neutral percent change from the vehicle of the radioligand in the presence of a fixed concentration (10 μ M) of each modulator under equilibrium conditions (Table S3). The radioligand bound was measured at 18 h, which ensures equilibrium ($k_{\text{on}} = k_{\text{off}}$) conditions were achieved.^{24,44} Thus, bars above the 0 line represent compounds that positively modulate radioligand binding as PAMs, possibly from increased agonist affinity. Bars significantly below the 0 line represent a net reduction in agonist radioligand binding, presumable due to competitive antagonism (**5**, **12a**, **13**, **17**, **18** and **28–36**). Only three (**28**, **35** and **36**) of these fourteen derivatives slowed agonist radioligand dissociation (Figure 1).²⁴

Comparing open-chain alkyl and fluorinated compounds **13–16**, the n -propyl derivative **13** decreased radioligand binding the most with a –45% change from the vehicle. Compound **14** increased radioligand binding the most with a 70% change from the vehicle.

Among the 2-cycloalkyl-substituted derivatives, compound **17** (2-cyclopropyl) decreased radioligand binding by 71% compared to the control, and compound **19** (2-cyclooctyl) increased radioligand binding by 41% compared to the control. Compounds **6–8** and **21–23** did not produce a net change in radioligand equilibrium binding compared to the control.

Among the bridged compounds, i.e., **12a**, **12b** and **24–29**, compounds **12b** (2-adamantan-1-yl), **26** (2-bicyclo[3.3.1]nonan-1-yl), and **27** (2-((1*R*,3*S*,5*S*)-bicyclo[3.3.1]nonan-3-yl)) significantly increased radioligand binding with a 19%, 38% and 41% change from vehicle, respectively. Compounds **24** and **25** had no effect on radioligand binding, while compounds **12a**, **28** and **29** decreased radioligand binding with –19%, –37% and –21% change from vehicle, respectively.

All the derivatives with hydrophilic substitutions, **30–34**, decreased A₃AR radioligand binding at equilibrium, with compound **33** having the most significant decrease in binding with a 36% change from vehicle when compared to the control (*P*-value = 0.023).

Of the *p*-substituted phenylamino derivatives, compound **37** increased agonist equilibrium binding the most with a 15% change from the vehicle. Compounds **35** and **36** decreased agonist equilibrium binding with –31% and –49% change from the vehicle, respectively. Compounds **38** and **39** did not affect radioligand binding at equilibrium compared to control.

In addition to the kinetic binding studies, the ability of each compound to allosterically modulate hA₃AR-dependent G protein activation by agonist **52** was measured in the [³⁵S]GTPγS functional assay (Figure 3 and Table S4). Concentration–response curves were generated for each compound, including a curve for the control (agonist **52** with DMSO) and curves for the agonist **52**.²⁴ Compounds **12a** and **12b** were reported in Kim et al.²⁰ and re-assayed here with a new protocol.

The effect on [³⁵S]GTPγS binding of each modulator (**5–8** and **12–39**) at concentrations of 0.1, 1.0, and 10 μM was determined (Tables 1 and S4, Figure 3). Compounds **7**, **14**, **18** and **20** were particularly efficacious and at least doubled the agonist *E*_{max} compared to control. Comparing the progression of effects of *N*-(3,4-dichlorophenyl)-1*H*-imidazo[4,5-*c*]quinolin-4-amine derivatives at 1.0 μM, there was a trend to increase the *E*_{max} from the 2-cyclopropyl derivative **17** to the 2-cyclononyl derivative **20**, except for 2-cyclo-octyl **19**. While not significant, there was a 2-fold increase in agonist potency in the presence of 1 μM of 2-cyclononyl derivative **20** compared to the agonist alone (*P*-value = 0.3712, one-way ANOVA with multiple comparisons). As the ring size increased from 2-cyclodecyl **21** to 2-cyclododecyl **23**, there was no change in agonist potency but a steady decrease in its *E*_{max}. The fluorinated compounds, **15** and **16**, at 1 μM moderately improved agonist *E*_{max} but did not influence agonist potency.

Of the bridged derivatives, **12b** and **26** at 1 μM enhanced the efficacy of agonist **52** to the greatest extent, having an *E*_{max} of 237 ± 12 and 219 ± 16 (*P*-value = 0.0002 and 0.0005, respectively). While neither **12b** nor **26** significantly improved agonist potency, **12b** at 1.0 μM tended to improve potency almost 4-fold from 46 nM to 10 nM (*P*-value = 0.058). Compounds **12a**, **24**, **27** and **28** moderately enhanced the [³⁵S]GTPγS binding in

the presence of agonist **52** compared to control. 2-(Bicyclo[2.2.1]heptan-1-yl) derivative **25** was the only bicyclic compound to induce a decrease in agonist potency at 1 μM (4-fold compared to the control, P -value = 0.0257). Compound **29** did not influence agonist potency and led to a moderate increase in agonist E_{max} (167 ± 12). All bicyclic compounds tended toward inverse agonist activity, and compound **29** at 10 μM decreased the basal efficacy the most, by $\sim 100\%$, at the lowest agonist concentration.

The derivatives with hydrophilic substitutions, compounds **30–34**, moderately allosterically enhanced [^{35}S]GTP γS binding (Figure 3 and Table S4). However, these modulators at concentrations of 0.1 μM and 1.0 μM had no significant effect on agonist potency compared to the control. At 1.0 μM , only compounds **31**, **32**, and **34** increased agonist E_{max} compared to the control, ranging from 167% to 186% maximal efficacy of the agonist alone. Like compound **29**, compound **34** behaved as an inverse agonist at 10 μM , decreasing basal efficacy at the lowest agonist concentration by $\sim 50\%$. The decreased lipophilicity of **34** relative to 2-cyclononyl derivative **20** was predicted using Stardrop software⁴⁵ with the following parameters for **34**: Log D = 5.53, topological polar surface area (TPSA) = 73.8 \AA^2 , and blood–brain barrier (BBB) $\log([\text{brain}]:[\text{blood}]) = -0.442$, i.e., not BBB penetrant. The same parameters for **20** were Log D = 7.08, TPSA = 53.6 \AA^2 , and BBB $\log([\text{brain}]:[\text{blood}])$ ratio = -0.0326 , i.e., BBB penetrant. Efficacious PAMs **14**, **18** and **39** were also predicted to penetrate the BBB. The calculated parameters for all compounds tested pharmacologically are provided in Table S5.

Of the *p*-substituted phenylamino derivatives, compounds **35**, **37**, and **38** at 1.0 μM moderately increased agonist efficacy compared to control (Figure 3 and Table S4). At 1 μM , compound **36** doubled the agonist efficacy compared to control. None of the *p*-substituted phenylamino derivatives influenced agonist potency compared to control. Compound **39** combined the favorable features of compounds **14** and **35**, based on their favorable modulation of dissociation kinetics and [^{35}S]GTP γS binding. Compound **39** contains both the 2-heptan-4-yl substitution of **14** and the 4-iodophenyl substitution of **35**. Compared to the control, compound **39** at 1 μM did not improve agonist potency but doubled agonist E_{max} .

The off-target screening was performed by the NIMH Psychoactive Drug Screening Program (PDSP) (Table 2).⁴⁶ A total of ten derivatives were tested for off-target binding activity against 45 other receptors, transporters, and channels. Only a few weak off-target interactions were observed, the lowest K_i being for compound **39** at the translocator protein (TSPO) with $K_i = 0.123 \mu\text{M}$. The two 4-iodophenyl derivatives tested, compounds **35** and **39**, were the only derivatives interacting with TSPO. Most derivatives interacted with one or two sigma receptors, specifically σ_1 and σ_2 . Compound **39** had the lowest K_i observed, 0.891 μM , among the derivatives interacting with a sigma receptor. Compound **27** interacted with the most off-target sites: κ (KOR) and μ (MOR) opioid receptors, σ_1 , σ_2 , dopamine transporter (DAT), and serotonin 5HT_{2B} receptors, interacting most strongly with DAT at $K_i = 0.467 \mu\text{M}$.

Experimental ADMET Properties.

We chose 2-cyclohept-4-enyl **18** and 2-heptan-4-yl-*N*-4-iodophenyl **39** derivatives as relatively potent (estimated) and efficacious A₃AR PAMs having only weak off-target interactions, to assess the pharmacological and ADMET properties in vivo and in vitro, as determined by reported methods.⁴⁷ In fasted Wistar rats, the plasma concentration of **18** and **39** was determined following three different doses administered by oral gavage (p.o.) or one dose administered intravenously (i.v.). Multiple in vitro assays assessed drug metabolism and pharmacokinetics (DMPK): plasma stability, HepG2 cytotoxicity, human ether-à-go-go-related gene (hERG) potassium channel inhibition, cytochrome P450 (CYP) inhibition, microsomal stability, pION solubility, plasma protein binding, and chemical stability in simulated gastric and intestinal fluids.

In vitro and in vivo pharmacokinetic parameters of compounds **18** and **39** are shown in Table 3 and Tables S6 and S7. When dissolved in simulated intestinal and gastric fluids, 88.1% and 69.1% of compound **18** remained after 2 h, respectively, and **39** was more stable in gastric fluid. Out of the five CYP enzymes tested, the inhibition with CYP1A2 was the most concerning, with IC₅₀ values of 6.99 (**18**) and 1.31 (**39**) μM. Both compounds had IC₅₀ values above 30 μM for the other four CYP enzymes measured. The plasma stability was satisfactory, with compound **18** having 88.7% remaining in rat plasma after 120 min. The highest half-life of compound **18** in plasma was achieved in the mouse plasma at 695 min. Both compounds were relatively stable in liver microsomal assays, having the most degradation with rat microsomes, i.e., 52% of **18** remaining after 120 min. In the microsomal stability assays, compound **18** had a greater % remaining in all species than the reference compound, testosterone. In the hERG potassium ion channel inhibition assay, compounds **18** and **39** displayed IC₅₀ values of 6.06 and >30 μM, respectively. Both compounds were not toxic to HepG2 liver cells, evidenced by an IC₅₀ greater than 30 μM. In all three species, human, rat, and mouse, compound **18** was strongly bound to plasma protein, having % bound values of ~100, 99.1, and ~100, respectively. **39** was less water-soluble but had a much higher free fraction (93.6% bound) than **18** in human plasma. The measured concentration of compound **18** in the pION solution buffer (pH 7.4) was 0.39 μg/mL (0.92 μM), i.e., low aqueous solubility.

Caco-2 permeability assay assessed intestinal permeability of compounds **18** and **39** (Table S7). Compound **18** had no measurable permeability (P_{app}) for either apical to basolateral (A to B) and basolateral to apical (B to A) and was therefore classified as having low permeability. An efflux ratio was not calculated due to low P_{app} in A to B and B to A. B to A had a relatively large % recovery of 78.0%, which was substantially more than the 48.1% seen for the A to B % recovery.

A comparison of the in vivo pharmacokinetics of **18** and **39** (Figure 4, Table 3, Table S8), indicated that **39** had considerably longer in vivo half-life and improved oral bioavailability (3.44 h, 64.0%F at 3 mg/kg; 3.84 h, 61.5%F at 10 mg/kg) than **18**, indicating substantial oral bioavailability. The longest half-life of 2.60 h of **18** was with an oral dose of 10 mg/kg, similar to the half-life of 2.38 h seen with the i.v. dose of 0.5 mg/kg **18**. 28.7%F and 47.5%F were determined for compound **18**. The source of the discrepancy between the low passive

drug absorption predicted using Caco-2 cells⁴⁸ and the moderate oral bioavailability remains unexplored.

An oral dose of 10 mg/kg of compound **18** produced higher plasma concentrations (C_{\max} at 2 h of 1780 ng/mL, equal to 4.2 μM) compared to the other groups during each time point measured. All groups of rats administered compound **18** orally, i.e., at 1, 3, and 10 mg/kg, achieved the maximum plasma concentration at ~ 2 h. However, other parameters were similar for **18** and **39**. Rats given 3 mg/kg had almost double the clearance rate (1580 mL/(h·kg)) of compound **18** from the plasma compared to 10 mg/kg (975 mL/(h·kg)) and roughly three times the clearance rate compared to 1 mg/kg (447 mL/(h·kg)) (Table S8). A 3 mg/kg dose had double the elimination rate constant, k_{el} , compared to other p.o. doses, having $\sim 50\%$ of the remaining compound in the body excreted every h. A 3 mg/kg dose produced the longest mean residence time (MRT, length of time a compound remains in the system before elimination) of 3.98 h.

Molecular Modeling.

In general a mixture of positive and negative modulatory hA₃AR effects was observed for this class of PAMs, with the negative modulation likely due to competitive antagonism at the orthosteric site.²⁴

As reported in Fisher et al.,²⁴ the 2-cyclopropyl analogue **17** was proposed to function predominantly as a competitive antagonist of the orthosteric site of the hA₃AR, because it retained the ability to right-shift the concentration–response curve of agonist **52** in [³⁵S]GTP γ S binding assays with a chimeric mouse_{in}/human_{out} A₃AR that is non-responsive to the efficacy-enhancing effect of the imidazoquinolinamine PAMs. Chimeric receptor studies proved that compound **7** interacts with both the allosteric and the orthosteric site. The binding affinity (K_{B}) of **17** for the orthosteric site of the chimeric receptor was estimated by Schild analysis to be 140 nM (Figure S1B). The affinity of **7**, which also reduces potency of Cl-IB-MECA in [³⁵S]GTP γ S binding assays at the mouse_{in}/human_{out} A₃AR, was estimated to be 799 nM at this chimeric receptor (Figure S1A). This conclusion was further supported in equilibrium binding studies with the antagonist radio-iodinated ligand [¹²⁵I]2-(4-(3-(4-amino-3-iodobenzyl)-2,6-dioxo-1-propyl-2,3,6,7-tetrahydro-1*H*-purin-8-yl)phenoxy)-acetic acid ([¹²⁵I]I-ABOPX), where **7** and **17** were found to displace specific binding to the WT hA₃AR (Figure S2). Compounds **7** and **17** were roughly equipotent in inhibiting orthosteric radioligand binding ($K_{\text{i}} \approx 2.0 \mu\text{M}$), whereas compound **14** was slightly less potent ($\sim 5.40 \mu\text{M}$). Compound **17** did not inhibit orthosteric antagonist binding to the hA₁, hA_{2A}, or hA_{2B} ARs at concentrations as high as 10 μM (Supporting Information).

Molecular modeling studies to rationalize the PAM activity and predict the allosteric binding site(s) are still ongoing and not part of this study, because further pharmacological characterization is needed. A PAM-bound hA₁AR experimental structure (PDB ID: 7LD3) is available,⁶ with 2-amino-4-(3,5-bis(trifluoromethyl)phenyl)thiophen-3-yl(4-chlorophenyl)-methanone (MIPS521, an hA₁AR PAM) bound to an intramembrane region at the interface among TM1, TM6, and TM7. Homology modeling of hA₃AR using structure 7LD3⁶ as

template (46% hA₁AR and hA₃AR sequence identity, computed with GPCRdb),⁶⁶ followed by docking of compound **7** to a binding pocket equivalent to the site of MIPS521 in the A₁AR, did not provide any reasonable poses (data not reported). This is possibly due to a more hindered pocket in hA₃AR, where the bulkier A273^{7.44} and M276^{7.47} replace the non-conserved G279^{7.44} and A282^{7.47} of hA₁AR (alignment reported in Figure S3). This, together with ongoing pharmacological experiments,²⁴ suggests that hA₁AR and hA₃AR allosteric sites are distinct, at least for MIPS521 at hA₁AR and the series of compounds of this manuscript at hA₃AR.

Conversely, we could model the ability of **17** to be accommodated in hA₃AR orthosteric site, which is well known for ARs. Given the lack of an experimental hA₃AR structure, we employed a previously reported homology model built on the experimental structure of an antagonist-bound hA₁AR X-ray structure.⁴⁹ The compound was docked to the orthosteric site through an induced fit docking (IFD) procedure⁵⁰ and refined by minimization through molecular mechanics with a generalized Born and surface area solvation (MM-GBSA).⁵¹ The selected hA₃AR pose of compound **17** (Figure 5) was compared to other known A₃AR ligands. In the suggested binding mode, the compound's 1*H*-imidazo[4,5-*c*]pyridin-4-amine moiety mimics the adenine scaffold of adenosine-like agonists⁴⁷ and the [1,2,4]triazolo[1,5-*c*]pyrimidin-5-amine scaffold of the known antagonist *N*-(9-chloro-2-(furan-2-yl)-[1,2,4]triazolo[1,5-*c*]quinazolin-5-yl)-2-phenylacetamide (**64**, MRS1220) in its previously predicted pose.⁴⁹ A conserved π - π stacking interaction is observed between the aromatic scaffold of **17**, similar to **64**, and F168^{EL2}, while nitrogen N3 and the exocyclic amino group at position 4 are engaged in a bidentate H-bond with N250^{6.55}. The 2-cyclopropyl moiety is located deep into the orthosteric binding pocket, surrounded by T94^{3.36}, M177^{5.38}, S181^{5.42}, I186^{5.47}, W243^{6.48}, L246^{6.51}, and N250^{6.55} (residues located within 3 Å), while the 3,4-dichlorophenyl group points toward the extracellular portion of the receptor, surrounded by the tip of TM6, TM7, EL2, and EL3, and specifically by residues Q167^{EL2}, F168^{EL2}, I249^{6.54}, N250^{6.55}, I253^{6.58}, V259^{EL3}, L264^{7.35}, and I268^{7.39}.

Considering that compound **7** shares with **17** the ability to inhibit orthosteric antagonist radioligand binding, we assessed its ability to fit the orthosteric binding pocket. We applied induced fit docking and MM-GBSA minimization and selected by visual inspection a possible orthosteric binding mode. Poses with the dichlorophenyl group anti respect to atom C5 (Figure S4B) were discarded as they are less favored and require overcoming a high energy barrier, as suggested by a dihedral scan performed with the semiempirical quantum mechanical methods GFNn-xTB (Figure S5). Compound **7** was thus predicted to bind the hA₃AR orthosteric binding pocket similarly to compound **17** (Figure S4A), which is in agreement with the experimentally demonstrated antagonist effect of the two compounds. This suggest that the two compounds' differential ability to enhance agonist activity (present for **7** and absent for **17**) is not due to a major antagonist character of **17** as compared to **7**, since their antagonist behavior is similar, but to a major PAM effect of compound **7**.

This study extended previous SAR studies of hA₃AR PAMs having an imidazoquinolinamine scaffold.^{14,52} A ligand structure-guided design approach was pursued given that structural information for the A₃AR is not yet available to enable a target-guided structural approach for PAMs. Although modeling predictions can be made for ligand

recognition at the hA₃AR orthosteric binding site by close similarity to the hA₁AR and hA_{2A}AR,⁵³ prediction of the precise allosteric ligand binding site is uncertain.

This class of PAMs is selective for the A₃AR with respect to allosteric modulation at other AR subtypes.^{18–20,22} However, a mixture of positive and negative modulatory A₃AR effects is generally observed in this family. The relatively low competitive binding of **4** and **7**^{19,20} and the lack of allosteric enhancement by **4** and **7**^{17,54} at other AR subtypes were reported. Based on chimeric receptors, we now know that the site of PAM action is on the cytosolic side of the receptor, while the negative effects in this series appear to arise from the canonical orthosteric site binding.²⁴ The A₃AR orthosteric antagonism by 2-cyclopropyl derivative **17** and prototypical A₃AR PAM **7** was quantified here using functional data from the mouse_{in}/human_{out} chimeric A₃AR and radioligand binding at the WT receptor,²² and their orthosteric binding was modeled. The ability of these derivatives and compound **14** to bind to varying degrees to the orthosteric site is also consistent with the fact that this 1*H*-imidazo[4,5-*c*]quinolin-4-amine scaffold was initially characterized as potent A₁AR antagonists.⁵⁵ Curiously, the topical anti-tumor agent imiquimod, which contains the same scaffold, was reported to antagonize ARs with μ M affinity.⁵⁶

Like past studies, this series of derivatives showed variable allosteric modulatory effects, with positive effects on [¹²⁵I]**50** dissociation, potency and/or maximal efficacy of **52** in functional assays. Although PAM effects were demonstrated here with synthetic agonists [¹²⁵I]**50** and **52**, the enhancing effects apply similarly to endogenous adenosine, as **7** increased the maximal efficacy of adenosine in [³⁵S]GTP γ S binding.²⁴

Prior 2-(*n*-pentyl) substitution (**9**) of the 1*H*-imidazo[4,5-*c*]quinolin-4-amine scaffold with the 3,4-dichlorophenylamino group at the 4 position did not significantly enhance A₃AR activity.¹⁹ However, another acyclic analogue, 2-heptan-4-yl derivative **14**, originating from the synthetic precursor valproic acid, at 1 μ M, enhanced agonist E_{\max} compared to control ($E_{\max} = 216 \pm 12\%$, P -value < 0.0001). This 2-fold increase in E_{\max} of **52** at the receptor was comparable to the enhancement by 2-cyclohexyl derivative **7**. Yet, it did not increase agonist potency compared to the control (P -value = 0.2041). Thus, for the first time we demonstrated that acyclic alkyl substitutions at the 2 position provides pharmacological advantages.

Other PAMs that significantly enhanced agonist efficacy at 0.1 μ M were **7**, **8**, **12b**, **16**, **18**, **20**, **27**, **37** and **39** (Table S4). When evaluating other cycloalkyl derivatives compared to compound **7**, compounds **18** (2-cyclohept-4-enyl), and **20** (2-cyclononyl) stand out. Both potentiated the maximal efficacy of agonist **52** similarly to compound **7** ($225 \pm 10\%$) at 1 μ M, having E_{\max} values of $241 \pm 9\%$ and $242 \pm 9\%$, respectively. Compounds **18** and **20** also showed PAM characteristics by slowing the rate of agonist radioligand dissociation from the receptor.

Use of bridged alicyclic rings at the 2 position for steric constraint failed to identify a hypothetical receptor-preferred conformation. All bridged modulators at 1 μ M increased agonist efficacy, with an approximately 2-fold increase by compounds **12b**, **24** and **28**. The tricyclic 2-(adamantan-1-yl) substitution enhanced agonist E_{\max} and trended toward

increasing potency (P -value = 0.058). Thus, none of the bicyclic derivatives improved agonist potency compared to control in the [^{35}S]GTP γS assay, but uniformly acted as PAMs by slowing the radioligand dissociation and improving the maximal efficacy of the agonist. The binding of bridged derivatives at both the orthosteric and allosteric binding sites is the most likely explanation for lack of substantial improvement in agonist potency. Another potential explanation is that the activation and binding cooperativities of these compounds are separate parameters controlling both agonist E_{max} and potency changes. Interestingly, the effect on agonist EC_{50} of bicyclic alkene **29** was similar to competitive antagonist **17**, significantly decreasing the potency in a concentration-dependent manner.

We installed different hydrophilic groups on compound **18** to potentially improve PAM water solubility while maintaining enhancement of the agonist dissociation and functional effects at the A_3AR . These derivatives with various oxygen substitutions (i.e., oxirane, alcohol, and carbonyl groups) did not influence agonist potency, but had similar improvements in agonist efficacy compared to the bicyclic library of derivatives. Thus, they act as PAMs,⁵⁷ but with limited cooperativity due to their mediocre slowing of radioligand dissociation, and they reduced radioligand binding at equilibrium, suggestive of orthosteric site binding.⁵⁸ Although efficacy enhancement compared to control was moderate, these derivatives were the first example of A_3AR PAM activity with any hydrophilic substitution, in light of the failure of previously tested polar heterocyclic derivatives.²⁰

In prior studies, certain halogenated and 4-substituted phenylamino derivatives were tolerated with respect to A_3AR PAM effects.²⁰ Overall, all p -phenylamino substitutions were tolerated here, but none having exceptional binding or functional effects compared to compound **7**. At $1\ \mu\text{M}$ concentration, potency remained unchanged and E_{max} doubled. Compounds **35** and **36**, with the 4-iodo- and 4-bromophenylamino substitutions, respectively, had a similar non-optimal influence on potency and efficacy as compounds **37** and **38**; though, they both considerably slowed the radioligand dissociation (58% and 56% remaining, respectively) compared to control (P -values = 0.010 and 0.015, respectively). Although compounds **35** and **36** slowed radioligand dissociation, they both considerably decreased the radioligand binding at equilibrium by 31% and 49% compared to the vehicle (P -values = 0.040 and 0.036, respectively). Thus, **35** and **36** bound to both orthosteric and allosteric sites, with greater inhibition of radioligand binding compared to other PAMs. Important to note is the substantial increase in agonist E_{max} at $1\ \mu\text{M}$ between compounds **35** and **39**, ($184 \pm 9\%$ and $223 \pm 10\%$, P -value = 0.044), correlating with the 2-heptan-4-yl substitution of **39**, which was also evident in improved equilibrium radioligand binding.

Interestingly, compound **37**, having a methyl acrylate p -phenylamino substitution, slowed radioligand dissociation and had favorable equilibrium binding results, with low % competitive inhibition of radioligand binding at the orthosteric binding site. These are promising results because **37** has more hydrophilic character (predicted $\text{Log } D = 5.12$, $\text{TPSA} = 79.7\ \text{\AA}^2$, and $\text{BBB } \log([\text{brain}]:[\text{blood}]) = -0.450$, i.e., not BBB penetrant) than the rest of the library due to the 4-aminophenyl substitution. Of the compounds with hydrophilic substitutions, compound **37** most represents a PAM. A hydrophilic p -phenylamino substitution might achieve a hydrophilic PAM, suggested by the differences in SAR between **37** and the derivatives with hydrophilic substitutions at the 2 position.

Altogether, it would be worth investigating the effects of other polar *p*-phenylamino substitutions.

Compounds **18** and **39** proved to be orally bioavailable, despite having low A-B and B-A permeability in Caco-2 cells. Neither was strongly depleted by simulated digestive fluid, while **39** and to a lesser extent **18** inhibited CYP1A2. **18** displayed extremely high plasma protein binding in all three species tested, attributed to its hydrophobic nature. It is conceivable that the high plasma protein binding could provide a reservoir of the PAM in the body for prolonged activity, as it would release gradually from a bound to unbound state. On the other hand, this could limit the amount of compound available to traverse to the cellular environment for event- and site-specific action.

CONCLUSIONS

This study aimed to further explore the SAR of A₃AR PAMs and to determine the suitability of the new analogues for translational development. We achieved our objectives of creating a shorter 6-step synthetic route for 1*H*-imidazo[4,5-*c*]quinolin-4-amine PAM derivatives, preparing a new series of 1*H*-imidazo-[4,5-*c*]quinolin-4-amine PAM derivatives, determining the SAR of the series of derivatives, and obtaining the first reported baseline ADMET of this structural family.

Although we did not discover a PAM derivative that induced a greater agonist efficacy-enhancement than compound **7**, we did reveal a trend toward higher efficacy with certain 2- and 4-amino substitutions, including **12**, **14**, **18**, **20**, **30**, and **39**. The heptan-4-yl 2 position substitution slowed agonist dissociation from the A₃AR the most, with both 3,4-dichlorophenyl and 4-iodophenyl substitutions at the 4-amino position. In addition to the 2-heptan-4-yl substitution, the 2-cyclohept-4-enyl and 2-cyclononyl substitutions improved agonist efficacy comparable to the reference 2-cyclohexyl. Other 2 position substitutions such as bicyclic and hydrophilic groups did not significantly enhance PAM effects, although these hydrophilic substitutions were more successful than previous attempts to introduce polar groups.

The human/mouse chimeric A₃AR data showed the dependence on the 2 position substitution of orthosteric site affinity, which is spatially distinct from the allosteric binding site located on the cytosolic half of the receptor. Thus, fine-tuning of this family of PAMs is achievable, by separating distinct orthosteric (undesired) and allosteric binding effects. These separate activities could be further probed using the chimeric A₃ARs as screening tools.

Developing a radioligand specific for the 1*H*-imidazo[4,5-*c*]quinolin-4-amine PAM binding site would significantly aid the pharmacological characterization of this PAM family. We prepared a precursor for introducing a ¹²⁵I label and will perform future labeling studies.

Thus, we have developed a series of 1*H*-imidazo[4,5-*c*]quinolin-4-amine modulators with promising characteristics. Selected compounds will be utilized in future preclinical studies once an animal disease model is identified, furthering the allosteric approach to developing drugs to activate the A₃AR that are event- and site-specific in action.

EXPERIMENTAL METHODS

Reagents and Instrumentation.

All glassware and stir bars were oven-dried before use in a reaction. All reactions were conducted in a ventilated hood. Pyrophoric reagents were handled and administered under a nitrogen gas atmosphere to reactions in an evacuated oven-dried glass round-bottom flask. Room temperature (rt) refers to 25 ± 5 °C. All final compounds were stored at 4 °C in a parafilm-sealed vial. Unless otherwise stated, all the reagents and solvents were purchased from Sigma-Aldrich (St. Louis, MO). Unless noted, the reagents and solvents were of reagent grade and used without further purification. The following suppliers supplied the following commercial compounds: TCFH was purchased from TCI (Portland, OR), bicyclo[3.3.1]nonane-1-carboxylic acid was purchased from Chemspace US (Monmouth Junction, NJ); bicyclo[3.3.1]nonane-3-carboxylic acid was purchased from AstaTech (Bristol, PA); cyclohept-4-ene carboxylic acid was purchased from Ambeed (Arlington Heights, IL); bicyclo[2.2.1]heptane-1-carboxylic acid was purchased from Enamine (Kyiv, Ukraine). All reagents used were of commercial grade.

NMR spectra were recorded on a Bruker 400, 500, or 600 MHz spectrometer at 25 °C under an optimized parameter setting for each sample (Supporting Information). For compounds **14**, **17**, **18–22**, **24–39**, **48**, and **49** ^1H NMR chemical shifts were measured relative to the residual solvent peak of 7.26 ppm for CDCl_3 or $\text{CDCl}_3/\text{CD}_3\text{OD}$. For compounds **15** and **23**, ^1H NMR chemical shifts were measured to the residual solvent peak of 2.5 ppm for $\text{DMSO}-d_6$. For compound **13**, ^1H NMR chemical shifts were measured to the residual solvent peak of 3.34 ppm for CD_3OD . For compounds **16**, ^1H NMR chemical shifts were measured to the residual solvent peak of 1.94 for CD_3CN . ^1H NMR chemical shifts were measured relative to tetramethylsilane at 0.00 ppm in CDCl_3 and the residual water peak at 3.30 ppm in CD_3OD . ^{19}F NMR spectra were recorded for derivatives **15**, **16**, and **20–23**.

Analytical TLC was performed on 0.2 mm silica-coated sheets with an F254 indicator (Sigma-Aldrich). TLC visualization of the products was aided using UV light or by staining with a solution of potassium permanganate (1.5 g of KMnO_4 , 10 g K_2CO_3 , and 1.25 mL 10% NaOH in 200 mL water). Column chromatography was performed on 230–400 mesh silica gel (pore size of 60 Å, Sigma-Aldrich).

Accurate mass data were obtained using a Xevo G2-XS QToF mass spectrometer (Supporting Information). The instrument was operated in positive-ion ESI mode at a resolution of 25,000. The ESI capillary voltage was 2.8 kV and the desolvation temperature was 280 °C. Accurate masses were determined using trifluoroacetic acid (TFA) sodium salt as an internal standard. An Acquity I-class Ultra Performance Liquid Chromatography (Waters, Milford, MA) was the liquid chromatography system. Solvent A was 100% water and solvent B was an 80:20 mixture of ACN:MeOH with 0.1% TFA and 0.2% formic acid added. The column was a ProSwift RP-4H 1×50 mm monolithic (ThermoFisher, Waltham, MA). The LC gradient was 0% B to 100% B in 10 min at a flow rate of 0.250 mL per min. Accurate mass high-resolution LC/ESI/MS at the Mass Spectrometry Facility, NIDDK, NIH.

HPLC analysis was carried out with Agilent 1100 Series HPLC equipped with Agilent Eclipse 5 μm XDB-C18 analytical column (250 \times 4.6 mm; Agilent Technologies Inc., Palo Alto, CA, USA). Mobile phase: linear-gradient solvent system, 10 mM TEAA (triethylammonium acetate): CH_3CN from 50:50 to 0:100 in 20 min, and then 100% CH_3CN for 5 min; the flow rate was 1.0 mL min, unless noted. The RP-HPLC was performed using a Phenomenex Luna 5 μm C18(2)100A, AXIA, 21.2 mm \times 250 mm column. The peaks were detected by UV absorption with a diode array detector at 210, 230, 254, and 280 nm. All derivatives tested for biological activity showed 95% purity in the HPLC systems, unless noted.

General Procedure for the Synthesis of Compounds 13–22.

Procedure C.—An oven-dried 10 mL round-bottom flask (cooled to rt under nitrogen) equipped with a stir bar was charged with the appropriate 2-substituted 4-chloro-1*H*-imidazo[4,5-*c*]quinoline derivative (**46a–n**) (1.0 equiv), 3,4-dichloroaniline (1.5 equiv), $\text{Pd}_2(\text{dba})_3$ (5–10 mol%), *t*BuXPhos (20 mol%), and sodium butoxide (1.5–2.0 equiv). The flask was evacuated for 2 min and backfilled with N_2 (gas). Dioxane (~1 mL) was added via syringe, and the reaction mixture was flushed/purged with nitrogen for 5 min while stirring. The reaction mixture was stirred at preheated oil bath (95–100 °C) under nitrogen for 16–24 h. Subsequently, the reaction mixture was cooled to rt and diluted with EtOAc (5 mL). The solution was then filtered through a silica plug. The filtrate was concentrated by rotary evaporation to obtain the crude product, purified by silica column with 10–25% ethyl acetate in hexane as the eluent system to obtain the product. Few products were further purified using reverse-phase high-pressure liquid chromatography.

2-Propyl-N-(3,4-dichlorophenyl)-1*H*-imidazo[4,5-*c*]quinolin-4-amine (**13**).—

Compound **13** was synthesized following the general procedure C described above using **46a** (15.0 mg, 0.061 mmol), $\text{Pd}_2(\text{dba})_3$ (5 mol%) and sodium *t*-butoxide (1.5 equiv). The crude was purified by silica gel column (10–20% ethyl acetate/hexane) to afford 6.0 mg (23%) of a white solid (HPLC t_{R} = 14.9 min): ^1H NMR (400 MHz, methanol-*d*₄) δ 8.60–8.55 (m, 1H), 8.00 (d, J = 8.1 Hz, 1H), 7.84 (dd, J = 19.6, 8.8 Hz, 2H), 7.55 (t, J = 7.9 Hz, 1H), 7.48–7.30 (m, 2H), 2.99 (t, J = 7.5 Hz, 2H), 1.96 (h, J = 7.4 Hz, 2H), 1.09 (t, J = 7.4 Hz, 3H); HRMS calcd for $\text{C}_{19}\text{H}_{17}\text{N}_4\text{Cl}_2$ ($\text{M}+\text{H}$)⁺ 371.0830, found 371.0827.

2-(Heptan-4-yl)-N-(3,4-dichlorophenyl)-1*H*-imidazo[4,5-*c*]quinolin-4-amine (**14**).—

Compound **14** was synthesized following the general procedure C described above using **46b** (26.0 mg, 0.086 mmol), $\text{Pd}_2(\text{dba})_3$ (5 mol%) and sodium *t*-butoxide (1.5 equiv). The crude was purified by silica gel column (10–20% ethyl acetate/hexane) to afford 4.2 mg (11%) of a white solid (HPLC t_{R} = 19.7 min): ^1H NMR (400 MHz, chloroform-*d*) δ 8.50 (d, J = 2.5 Hz, 1H), 8.01 (d, J = 8.4 Hz, 1H), 7.87–7.77 (m, 3H), 7.56 (t, J = 7.8 Hz, 1H), 7.44–7.30 (m, 2H), 3.03 (p, J = 7.3 Hz, 1H), 1.81 (td, J = 8.9, 8.3, 4.4 Hz, 4H), 1.43–1.26 (m, 4H), 0.92 (t, J = 7.3 Hz, 6H); HRMS calcd for $\text{C}_{13}\text{H}_{25}\text{N}_4\text{Cl}_2$ ($\text{M}+\text{H}$)⁺ 427.1456, found 427.1462.

2-(1,1,1,7,7,7-Hexafluoroheptan-4-yl)-N-(3,4-dichlorophenyl)-1*H*-imidazo[4,5-*c*]quinolin-4-amine (**15**).—

Compound **15** was synthesized following the general

procedure C described above using **46c** (4.8 mg, 0.012 mmol), Pd₂(dba)₃ (10 mol%) and sodium *t*-butoxide (2.0 equiv) gave **15** (3.2 mg, 50%) as a white solid. The crude was purified by silica gel column (10–20% ethyl acetate/hexane) followed by semipreparative HPLC (RP-HPLC linear gradient solvent system: ACN:H₂O from 80:20 to 100:0 in 40 min, at a rate of 5 mL/min. *t*_R = 29 min) to afford 3.2 mg (50%) of a white solid (HPLC purity: 91%; *t*_R = 18.1 min): ¹⁹F NMR (DMSO-*d*₆) δ -64.75; ¹H NMR (400 MHz, DMSO-*d*₆) δ 8.27–8.09 (m, 1H), 8.09–7.94 (m, 1H), 7.85 (s, 1H), 7.62 (d, *J* = 11.5 Hz, 2H), 7.49 (s, 2H), 2.34 (d, *J* = 14.0, 2H), 2.10 (d, *J* = 7.5 Hz, 6H); HRMS calcd for C₂₃H₁₉N₄F₆Cl₂ (M+H)⁺ 535.0891, found 535.0901.

2-(4-(Trifluoromethyl)cyclohexyl)-N-(3,4-dichlorophenyl)-1H-imidazo[4,5-c]quinolin-4-amine (16).—Compound **16** was synthesized following

the general procedure C described above using **46d** (14.0 mg, 0.040 mmol), Pd₂(dba)₃ (5 mol%) and sodium *t*-butoxide (2.0 equiv). The crude was purified by silica gel column (10–20% ethyl acetate/hexane) to afford 4.0 mg (21%) of a white solid (HPLC *t*_R = 18.2 min): ¹⁹F NMR (acetonitrile-*d*₃) δ -74.30; ¹H NMR (400 MHz, acetonitrile-*d*₃) δ 8.65 (d, *J* = 2.5 Hz, 1H), 8.14 (s, 1H), 8.01 (dd, *J* = 8.8, 2.6 Hz, 1H), 7.88 (d, *J* = 8.3 Hz, 1H), 7.55 (ddd, *J* = 8.4, 7.0, 1.5 Hz, 1H), 7.50–7.38 (m, 2H), 3.05–2.94 (m, 1H), 2.31 (d, *J* = 12.9 Hz, 2H), 2.13 (d, *J* = 22.1 Hz, 4H), 1.80–1.71 (m, 1H), 1.61–1.49 (m, 2H); HRMS calcd for C₂₃H₂₀N₄F₃Cl₂ (M+H)⁺ 479.1017, found 479.1019.

2-(Cyclopropyl)-N-(3,4-dichlorophenyl)-1H-imidazo[4,5-c]quinolin-4-amine (17).

—Compound **17** was synthesized following the general procedure C described above using **46e** (11.0 mg, 0.045 mmol), Pd₂(dba)₃ (10 mol%) and sodium *t*-butoxide (2.0 equiv). The crude was purified by silica gel column (10–20% ethyl acetate/hexane) to afford 3.0 mg (18%) of a white solid (HPLC *t*_R = 14.4 min): ¹H NMR (400 MHz, chloroform-*d*) δ 8.48 (s, 1H), 7.91 (d, *J* = 8.3 Hz, 1H), 7.86–7.71 (m, 2H), 7.48 (t, *J* = 7.6 Hz, 1H), 7.39–7.27 (m, 2H), 2.12 (p, *J* = 6.7 Hz, 1H), 1.14 (d, *J* = 6.5 Hz, 4H); HRMS calcd for C₁₉H₁₅N₄Cl₂ (M+H)⁺ 369.0674, found 369.0676.

2-(Cyclohept-4-en-1-yl)-N-(3,4-dichlorophenyl)-1H-imidazo[4,5-c]quinolin-4-amine (18).—Compound **18** was synthesized following the general procedure

C described above using **46j** (9.0 mg, 0.030 mmol), Pd₂(dba)₃ (10 mol%) and sodium *t*-butoxide (2.0 equiv). The crude was purified by silica gel column (10–20% ethyl acetate/hexane) to afford 3.0 mg (23%) of a white solid (HPLC *t*_R = 18.4 min): ¹H NMR (400 MHz, chloroform-*d*) δ 8.49 (s, 1H), 8.00 (d, *J* = 8.3 Hz, 1H), 7.79 (d, *J* = 8.4 Hz, 2H), 7.60–7.52 (m, 1H), 7.43–7.34 (m, 2H), 5.91 (dd, *J* = 4.9, 2.4 Hz, 2H), 3.27 (dq, *J* = 6.8, 3.3 Hz, 1H), 2.43 (d, *J* = 15.8 Hz, 2H), 2.37–2.20 (m, 4H), 1.85 (dt, *J* = 13.5, 10.9 Hz, 2H); HRMS calcd for C₂₃H₂₁N₄Cl₂ (M+H)⁺ 423.1143, found 423.1137.

2-(Cyclooctyl)-N-(3,4-dichlorophenyl)-1H-imidazo[4,5-c]quinolin-4-amine (19).

—Compound **19** was synthesized following the general procedure C described above using **46k** (40.0 mg, 0.13 mmol), Pd₂(dba)₃ (10 mol%) and sodium *t*-butoxide (2.0 equiv). The crude was purified by silica gel column (10–20% ethyl acetate/hexane) to afford 15 mg (27%) of a white solid (HPLC *t*_R = 20.5 min): ¹H NMR (400 MHz, chloroform-*d*) δ 8.43

(s, 1H), 8.04–7.65 (m, 3H), 7.61–7.47 (m, 1H), 7.46–7.29 (m, 2H), 3.27 (t, $J = 9.6$ Hz, 1H), 2.21–2.10 (m, 2H), 2.09–1.95 (m, 2H), 1.84 (s, 2H), 1.67 (s, 8H); HRMS calcd for $C_{24}H_{25}N_4Cl_2$ (M+H)⁺ 439.1456, found 439.1452.

2-(Cyclononyl)-N-(3,4-dichlorophenyl)-1H-imidazo[4,5-c]quinolin-4-amine (20).

—Compound **20** was synthesized following the general procedure C described above using **46l** (6.0 mg, 0.018 mmol), $Pd_2(dba)_3$ (10 mol%) and sodium *t*-butoxide (2.0 equiv). The product was obtained as a white solid (TFA salt) after lyophilization (2.0 mg, 5%; RP-HPLC, linear gradient solvent system: ACN:0.1% aq. TFA from 70:30 to 100:0 in 40 min, $t_R = 21.7$ min): ¹H NMR (400 MHz, chloroform-*d*) δ 8.01 (s, 1H), 7.68 (d, $J = 8.3$ Hz, 1H), 7.60–7.54 (m, 1H), 7.48 (s, 1H), 7.36 (s, 1H), 7.29 (dd, $J = 8.5, 2.5$ Hz, 2H), 3.29 (s, 1H), 1.97 (d, $J = 4.6$ Hz, 5H), 1.77–1.53 (m, 9H), 1.26 (s, 2H); HRMS calcd for $C_{25}H_{27}N_4Cl_2$ (M+H)⁺ 453.1613, found 453.1616.

2-(Cyclodecyl)-N-(3,4-dichlorophenyl)-1H-imidazo[4,5-c]quinolin-4-amine (21).

—Compound **21** was synthesized following the general procedure C described above using **46m** (13.0 mg, 0.038 mmol), $Pd_2(dba)_3$ (10 mol%) and sodium *t*-butoxide (2.0 equiv). The product was obtained as a white solid (TFA salt) after lyophilization (2.8 mg, 16%; RP-HPLC, linear gradient solvent system: ACN:0.1% aq. TFA from 70:30 to 100:0 in 40 min, at a rate of 5 mL/min; HPLC purity: 77%; $t_R = 23.8$ min): ¹H NMR (400 MHz, chloroform-*d*) δ 8.44 (s, 1H), 7.89 (d, $J = 8.4$ Hz, 2H), 7.74 (d, $J = 8.3$ Hz, 1H), 7.47 (t, $J = 7.8$ Hz, 1H), 7.37–7.27 (m, 2H), 3.53 (s, 1H), 2.05 (t, $J = 10.1$ Hz, 1H), 1.94 (s, 2H), 1.59 (s, 8H), 0.81 (s, 4H), 0.71–0.57 (m, 3H); HRMS calcd for $C_{26}H_{29}N_4Cl_2$ (M+H)⁺ 467.1769, found 467.1770.

2-(Cycloundecyl)-N-(3,4-dichlorophenyl)-1H-imidazo[4,5-c]quinolin-4-amine (22).

—Compound **22** was synthesized following the general procedure C described above using **46n** (14.0 mg, 0.039 mmol), $Pd_2(dba)_3$ (10 mol%) and sodium *t*-butoxide (2.0 equiv). The product was obtained as a white solid (TFA salt) after lyophilization (2.82 mg, 15%; RP-HPLC, linear gradient solvent system: ACN:0.1% aq. TFA from 70:30 to 100:0 in 40 min, at a rate of 5 mL/min; HPLC purity: 80%; $t_R = 22.7$ min): ¹H NMR (400 MHz, chloroform-*d*) δ 8.10 (s, 1H), 8.00 (d, $J = 8.0$ Hz, 1H), 7.85 (d, $J = 8.4$ Hz, 1H), 7.60–7.42 (m, 2H), 7.36 (d, $J = 9.0$ Hz, 2H), 3.19 (s, 1H), 1.88 (td, $J = 13.1, 12.7, 6.8$ Hz, 2H), 1.41 (d, $J = 11.0$ Hz, 6H), 1.27–1.14 (m, 10H), 0.78 (d, $J = 7.0$ Hz, 2H); HRMS calcd for $C_{27}H_{31}N_4Cl_2$ (M+H)⁺ 481.1926, found 481.1921.

General Procedure for the Synthesis of Compounds 23, 29, 35, 36, and 39.

Procedure E.—The appropriate 4-chloro-2-substituted 1*H*-imidazo[4,5-*c*]quinoline (**46b,h,o,t**) starting material (0.05 mmol, 1 equiv) and the appropriate halogenated aniline compound (**47a–c**) (0.15–0.25 mmol, 3–5 equiv) were added to 1 mL of ethanol in a 2 to 5 mL microwaveable vial. The reaction contents were degassed with $N_2(g)$ for 15 min, and the reaction was set up in an Initiator microwave reactor (Biotage, Charlotte, NC) at 130 °C for 6 h. The reaction mixture was filtered through a silica plug. The filtrate was evaporated in vacuo, and the product was purified by flash chromatography with a 15% ethyl acetate in hexane eluent system.

2-(Cyclododecyl)-N-(3,4-dichlorophenyl)-1H-imidazo[4,5-c]quinolin-4-amine (23).—Compound **23** was synthesized following the general procedure E described above using **46o** (6.0 mg, 0.016 mmol) and **47a** (13.0 mg, 0.08 mmol, 5.0 equiv). The product was obtained as a white solid (TFA salt) after lyophilization (2.0 mg, 25%; RP-HPLC acetonitrile/0.1% aq. TFA, 70/30 in 40 min at a rate of 5 mL/min, HPLC t_R = 21.6 min): ^1H NMR (400 MHz, DMSO- d_6) δ 8.22 (d, J = 7.4 Hz, 1H), 7.87 (s, 1H), 7.61 (s, 2H), 7.50 (s, 2H), 2.97 (s, 1H), 1.98 (s, 3H), 1.83 (s, 3H), 1.43 (d, J = 32.5 Hz, 17H), 1.27 (s, 3H); HRMS calcd for $\text{C}_{28}\text{H}_{33}\text{N}_4\text{Cl}_2$ (M+H) $^+$ 495.2082, found 495.2085.

General Procedure for the Synthesis of Compounds 24–27.

Procedure D.—To a 10 mL round-bottom flask (cooled to rt under $\text{N}_2(\text{g})$) equipped with a stir bar were added $\text{Pd}(\text{OAc})_2$ (1 mol%), *t*BuXPhos (3 mol%), and H_2O (40 mol %) and dissolved in 1.0 mL of 1,4-dioxane. The solution was degassed with nitrogen for 15 min and allowed to stir at 80 °C for 5 min. The appropriate 2-substituted 4-chloro-1*H*-imidazo-[4,5-*c*]quinoline derivative (**46p–s**) (1.0 equiv), 3,4-dichloroaniline (1.2 equiv), and sodium butoxide (2.0 equiv) were dissolved in 3 mL of dry 1,4-dioxane in a separate 25 mL round-bottom flask. The reaction mixture in the 25 mL round-bottom flask was degassed at rt with nitrogen for 15 min. The activated catalyst from the 10 mL flask was cooled and then transferred to the 25 mL reaction mixture using a cannula. The 25 mL flask was slightly immersed in a 100 °C oil bath, and the reaction continued for 16–20 h. The reaction mixture was diluted with ethyl acetate (5 mL) and filtered through a short silica plug. A rotary evaporator concentrated the filtrate to obtain a residue, purified by silica column chromatography with 10% ethyl acetate in hexane as the eluent system to afford the product.

2-(Bicyclo[1.1.1]heptan-1-yl)-N-(3,4-dichlorophenyl)-1H-imidazo[4,5-c]quinolin-4-amine (24).—Compound **24** was synthesized following the general procedure D described above using **46p** (47.0 mg, 0.17 mmol). The crude was purified by silica gel column (10–20% ethyl acetate/hexane) to afford 9.0 mg (13%) of a white solid (HPLC t_R = 16.1 min): ^1H NMR (400 MHz, chloroform-*d*) δ 8.47 (s, 1H), 8.00 (s, 1H), 7.80 (d, J = 24.6 Hz, 2H), 7.57 (s, 1H), 7.41 (d, J = 9.6 Hz, 2H), 2.68 (s, 1H), 2.40 (s, 6H); HRMS calcd for $\text{C}_{21}\text{H}_{17}\text{N}_4\text{Cl}_2$ (M+H) $^+$ 395.0830, found 395.0835.

2-(Bicyclo[2.2.1]heptan-1-yl)-N-(3,4-dichlorophenyl)-1H-imidazo[4,5-c]quinolin-4-amine (25).—Compound **25** was synthesized following the general procedure D described above using **46q** (383 mg, 1.29 mmol). The crude was purified by silica gel column (10–20% ethyl acetate/hexane) to afford 179 mg (33%) of a white solid (HPLC t_R = 18.3 min): ^1H NMR (400 MHz, chloroform-*d*) δ 8.49 (d, J = 2.6 Hz, 1H), 8.01 (d, J = 8.4 Hz, 1H), 7.82 (dd, J = 8.7, 2.7 Hz, 2H), 7.56 (ddd, J = 8.4, 7.0, 1.5 Hz, 1H), 7.43–7.34 (m, 2H), 2.53 (d, J = 4.8 Hz, 1H), 1.95–1.84 (m, 6H), 1.57 (d, J = 11.2 Hz, 2H), 1.26 (t, J = 7.1 Hz, 2H); HRMS calcd for $\text{C}_{23}\text{H}_{21}\text{N}_4\text{Cl}_2$ (M +H) $^+$ 423.1143, found 423.1140.

2-(Bicyclo[3.3.1]nonan-1-yl)-N-(3,4-dichlorophenyl)-1H-imidazo[4,5-c]quinolin-4-amine (26).—Compound **26** was synthesized following the general procedure D described above using **46r** (333 mg, 1.02 mmol). The crude was purified by silica gel column (10–20% ethyl acetate/hexane) to afford

101 mg (22%) of a white solid (HPLC t_R = 21.0 min): ^1H NMR (400 MHz, chloroform-*d*) δ 8.49 (d, J = 2.6 Hz, 1H), 8.00 (d, J = 8.4 Hz, 1H), 7.82 (dd, J = 11.5, 8.5 Hz, 2H), 7.55 (t, J = 7.7 Hz, 1H), 7.44–7.34 (m, 2H), 2.27–2.08 (m, 6H), 1.79 (q, J = 8.4, 6.6 Hz, 6H), 1.26 (t, J = 7.1 Hz, 3H); HRMS calcd for $\text{C}_{25}\text{H}_{25}\text{N}_4\text{Cl}_2$ ($\text{M}+\text{H}$) $^+$ 451.1456, found 451.1452.

2-((1R,3s,5S)-Bicyclo[3.3.1]nonan-3-yl)-N-(3,4-dichlorophenyl)-1H-imidazo[4,5-c]quinolin-4-amine (27).—Compound **27** was synthesized following the general procedure D described above using **46s** (255 mg, 0.78 mmol). The crude was purified by silica gel column (10–20% ethyl acetate/hexane) to afford 5.7 mg (2%) of a white solid (HPLC t_R = 19.4 min): ^1H NMR (400 MHz, chloroform-*d*) δ 8.47 (s, 1H), 8.00 (d, J = 8.4 Hz, 1H), 7.85–7.75 (m, 3H), 7.60–7.51 (m, 1H), 7.37 (t, J = 8.3 Hz, 2H), 3.23 (ddt, J = 19.1, 12.9, 5.7 Hz, 1H), 2.37 (td, J = 12.7, 5.7 Hz, 2H), 2.23 (d, J = 11.4 Hz, 2H), 1.93–1.81 (m, 2H), 1.72–1.62 (m, 3H), 1.51 (dd, J = 8.3, 4.8 Hz, 5H); HRMS calcd for $\text{C}_{25}\text{H}_{25}\text{N}_4\text{Cl}_2$ ($\text{M}+\text{H}$) $^+$ 451.1456, found 451.1460.

Synthesis of **28** by the Cyclopropanation of **18**.

2-((1R,4r,7S)-bicyclo[5.1.0]octan-4-yl)-N-(3,4-dichlorophenyl)-1H-imidazo[4,5-c]quinolin-4-amine (28).—2-(Cyclohept-4-en-1-yl)-*N*-(3,4-dichlorophenyl)-1*H*-imidazo[4,5-*c*]quinolin-4-amine (**18**, 30.0 mg, 0.071 mmol) was added to 1 mL of dichloromethane in a 10 mL round-bottom flask. The reaction mixture was cooled to 0 °C and degassed with $\text{N}_2(\text{g})$ for 15 min. Diethylzinc (249 μL , 0.25 mmol) was slowly added to the reaction vessel, followed by the slow addition of diiodomethane (29 μL , 0.35 mmol). The reaction mixture was stirred at 0 °C for 30 min and then the silicone stopper was replaced with a plastic stopper and wrapped with parafilm. The reaction mixture was stirred at rt overnight. Saturated ammonium chloride (0.5 mL) was added to the reaction vessel, and the reaction continued to stir for 30 min. The product was extracted with ethyl acetate, and the organic layer was washed with water (1 \times 5 mL) and brine (1 \times 5 mL). The organic layer was dried over magnesium sulfate, filtered, and concentrated by a rotary evaporator to obtain a residue purified by flash chromatography using 15% ethyl acetate in hexane eluent system to provide 4.0 mg (13%) of product as a white solid (HPLC t_R = 19.0 min): ^1H NMR (400 MHz, chloroform-*d*) δ 8.47 (s, 1H), 7.92 (d, J = 8.4 Hz, 1H), 7.86 (s, 1H), 7.79–7.72 (m, 1H), 7.50 (t, J = 7.7 Hz, 1H), 7.38 (d, J = 8.7 Hz, 1H), 7.31 (t, J = 7.5 Hz, 1H), 2.95–2.84 (m, 1H), 2.33 (dt, J = 13.3, 5.7 Hz, 2H), 2.17 (dt, J = 9.0, 5.3 Hz, 2H), 1.88 (q, J = 12.5 Hz, 2H), 1.13–1.00 (m, 2H), 0.95 (q, J = 7.3, 6.3 Hz, 2H), 0.86 (d, J = 7.7 Hz, 1H), 0.77 (td, J = 7.8, 4.5 Hz, 1H). HRMS calcd for $\text{C}_{24}\text{H}_{23}\text{N}_4\text{Cl}_2$ ($\text{M}+\text{H}$) $^+$ 437.1300, found 437.1304.

2-((1R,2R,4R)- and (1S,2S,4S))-Bicyclo[2.2.2]oct-5-en-2-yl)-N-(3,4-dichlorophenyl)-1H-imidazo[4,5-c]quinolin-4-amine (29).—Compound **29** was synthesized following the general procedure E described above using **46t** (8.0 mg, 0.026 mmol) and **47a** (13 mg, 0.077 mmol). The crude was purified by silica gel column (10–20% ethyl acetate/hexane) to afford 4.0 mg (36%) of a white solid (HPLC t_R = 17.9 min): ^1H NMR (400 MHz, chloroform-*d*) δ 8.50 (d, J = 2.6 Hz, 1H), 7.98 (d, J = 8.4 Hz, 1H), 7.75 (d, J = 8.1 Hz, 3H), 7.55 (ddd, J = 8.4, 7.0, 1.5 Hz, 1H), 7.44–7.33 (m, 2H), 6.70 (t, J = 7.5 Hz, 1H), 6.40 (t, J = 7.4 Hz, 1H), 3.47 (ddd, J = 10.3, 5.4, 2.1 Hz, 1H), 2.97–2.91 (m, 1H),

2.87–2.78 (m, 1H), 2.25 (ddd, $J = 13.1, 10.2, 2.7$ Hz, 1H), 1.86–1.76 (m, 1H), 1.71–1.62 (m, 2H), 1.49–1.34 (m, 2H); HRMS calcd for $C_{24}H_{21}N_4Cl_2$ (M+H)⁺ 435.1143, found 435.1136.

Synthesis of **30** and **31** by the Epoxidation of **18**.

m-Chloroperoxybenzoic acid (17.0 mg, 0.10 mmol, 2.0 equiv) was added to a 10 mL round-bottom flask containing a solution of 2-(cyclohept-4-en-1-yl)-*N*-(3,4-dichlorophenyl)-1*H*-imidazo[4,5-*c*]quinolin-4-amine **18** (21.0 mg, 0.05 mmol, 1.0 equiv) in 2 mL of dichloromethane. The reaction mixture was stirred at rt for 3 h. Once the starting material disappeared via TLC, 1 mL of acetone and 1 mL of 10% aq. sodium bicarbonate were added, and the mixture was allowed to stir for 30 min. The product was extracted with ethyl acetate (5 mL), and the organic layer was washed with water (10 mL) and brine (10 mL). The organic layer was dried using magnesium sulfate and then filtered. A rotary evaporator evaporated the solvent to obtain a crude residue, first purified by flash chromatography using a 30% acetone in hexane eluent system to obtain a mixture of **30** and **31**. A second flash chromatography column used a 0.75–1.0% methanol in dichloromethane eluent system to separate and isolate **30** (2.0 mg, 6%, red solid, analytical HPLC $t_R = 14.1$ min) and **31** (4.0 mg, 12%, red solid, analytical HPLC $t_R = 14.3$ min).

2-((1*R*,4*S*,7*S*)-8-Oxabicyclo[5.1.0]octan-4-yl)-*N*-(3,4-dichlorophenyl)-1*H*-imidazo[4,5-*c*]quinolin-4-amine (30**).**—¹H NMR (400 MHz, chloroform-*d*) δ 8.47 (s, 1H), 7.93 (t, $J = 8.7$ Hz, 2H), 7.76 (dd, $J = 8.7, 2.6$ Hz, 1H), 7.56–7.49 (m, 1H), 7.41–7.31 (m, 2H), 3.27 (dd, $J = 4.4, 1.8$ Hz, 2H), 2.71 (s, 1H), 2.46 (d, $J = 15.4$ Hz, 2H), 2.09–1.80 (m, 6H); HRMS calcd for $C_{23}H_{21}N_4OCl_2$ (M+H)⁺ 439.1092, found 439.1093.

2-((1*R*,4*r*,7*S*)-8-Oxabicyclo[5.1.0]octan-4-yl)-*N*-(3,4-dichlorophenyl)-1*H*-imidazo[4,5-*c*]quinolin-4-amine (31**).**—¹H NMR (400 MHz, chloroform-*d*) δ 8.50 (s, 1H), 7.94 (d, $J = 8.4$ Hz, 1H), 7.86 (d, $J = 8.0$ Hz, 1H), 7.79 (dd, $J = 8.9, 2.6$ Hz, 1H), 7.56–7.48 (m, 1H), 7.35 (dd, $J = 15.7, 8.2$ Hz, 2H), 3.15 (q, $J = 4.6$ Hz, 2H), 3.11–3.02 (m, 1H), 2.41 (dt, $J = 13.8, 6.4$ Hz, 2H), 2.14–2.05 (m, 3H), 2.01–1.88 (m, 3H); HRMS calcd for $C_{23}H_{21}N_4OCl_2$ (M+H)⁺ 439.1092, found 439.1090.

Synthesis of **32** by the Oxidation of a Mixture of Compounds **33** and **34**.

(*R*)- and (*S*)-4-(4-((3,4-dichlorophenyl)amino)-1*H*-imidazo[4,5-*c*]quinolin-2-yl)cycloheptan-1-one (**32**). A 10 mL round-bottom flask containing a solution of (1*R*,4*S*)-, (1*S*,4*R*)-, (1*R*,4*R*)-, and (1*S*,4*S*)-4-(4-((3,4-dichlorophenyl)amino)-1*H*-imidazo[4,5-*c*]quinolin-2-yl)cycloheptan-1-ol (17.0 mg, 0.039 mmol) **33**, and **34** in 1.5 mL dichloromethane, Dess–Martin periodinane (25.0 mg, 0.058 mmol) was added in one portion. The reaction mixture was stirred at rt until the starting material disappeared (monitored by TLC). The reaction mixture was quenched with saturated aq. $NaHCO_3$ (2 mL). The product was extracted with dichloromethane (5 mL) and the organic layer washed with water (10 mL) and brine (10 mL). The organic layer was dried over magnesium sulfate, filtered, and concentrated by rotary evaporator to obtain a crude residue, which was purified by flash chromatography using a 0.75 to 1.0% methanol in dichloromethane eluent system to provide 3.9 mg (23%) of compound **32** as a red solid (HPLC purity: 95%; $t_R = 13.2$ min): ¹H NMR (400 MHz, chloroform-*d*) δ 8.46 (s, 1H), 7.99 (d, $J = 8.4$ Hz, 1H), 7.79 (s, 2H),

7.60–7.53 (m, 1H), 7.42–7.34 (m, 2H), 3.27–3.18 (m, 1H), 2.77 (t, $J = 6.1$ Hz, 2H), 2.67 (q, $J = 5.1$ Hz, 2H), 2.38 (d, $J = 17.5$ Hz, 2H), 2.15 (td, $J = 12.9, 10.8, 7.3$ Hz, 2H), 2.04–1.88 (m, 2H); HRMS calcd for $C_{23}H_{21}N_4OCl_2$ (M+H)⁺ 439.1092, found 439.1100.

Synthesis of Hydroxy Derivatives **33** and **34** by the Hydroboration–Oxidation of **18**.

2-(Cyclohept-4-en-1-yl)-*N*-(3,4-dichlorophenyl)-1*H*-imidazo[4,5-*c*]quinolin-4-amine **18** (20 mg, 0.05 mmol, 1.0 equiv) was added to 0.5 mL of dry tetrahydrofuran (THF) in a 25 mL round-bottom flask and flushed with N₂(g). The reaction mixture was cooled to 0 °C, and borane dimethyl sulfide complex solution in 2.0 M THF (47 μL, 0.1 mmol) was added to the reaction vessel. The reaction mixture was stirred for 30 min at 0 °C and then overnight at rt. The reaction flask was placed in a 0 °C ice–water bath when all the starting material was consumed. 10% aq. NaOH (0.5 mL, 0.15 mmol) and H₂O₂ (1 mL, 0.26 mmol) were added successively to the reaction vessel. The reaction mixture reacted at 0 °C for 3 h. The product was extracted with ethyl acetate (5 mL), and the organic layer was washed with water (10 mL) and brine (10 mL). The organic layer was dried over magnesium sulfate, filtered, and then evaporated by a rotary evaporator. Compounds **33** (1.6 mg, 8%, red solid, analytical HPLC $t_R = 12.2$ min) and **34** (2.6 mg, 12%, red solid (analytical HPLC $t_R = 12.4$ min) were isolated and purified from the crude residue by flash chromatography using a 0.75–1.0% methanol in dichloromethane eluent system.

(1R,4S)- and (1S,4R)-4-(4-((3,4-Dichlorophenyl)amino)-1H-imidazo[4,5-c]quinolin-2-yl)cycloheptan-1-ol (33).—¹H NMR (400 MHz, chloroform-*d*) δ 8.47 (d, $J = 2.6$ Hz, 1H), 7.93 (t, $J = 7.7$ Hz, 2H), 7.77 (dd, $J = 8.8, 2.6$ Hz, 1H), 7.50 (ddd, $J = 8.4, 6.9, 1.5$ Hz, 1H), 7.38–7.28 (m, 2H), 4.06 (dq, $J = 9.3, 4.5$ Hz, 1H), 3.15 (tt, $J = 9.6, 4.4$ Hz, 1H), 2.22–2.03 (m, 3H), 2.00–1.79 (m, 5H), 1.63 (dddd, $J = 13.7, 10.3, 8.0, 2.1$ Hz, 1H), 1.52–1.39 (m, 1H); HRMS calcd for $C_{23}H_{23}N_4OCl_2$ (M+H)⁺ 441.1249, found 441.1247.

(1R,4S)- and (1S,4R)-4-(4-((3,4-Dichlorophenyl)amino)-1H-imidazo[4,5-c]quinolin-2-yl)cycloheptan-1-ol (34).—¹H NMR (400 MHz, chloroform-*d*) δ 8.48 (d, $J = 2.7$ Hz, 1H), 7.93 (d, $J = 8.3$ Hz, 1H), 7.87 (d, $J = 7.9$ Hz, 1H), 7.78 (dd, $J = 8.8, 2.6$ Hz, 1H), 7.50 (ddd, $J = 8.4, 6.9, 1.5$ Hz, 1H), 7.40–7.28 (m, 2H), 3.97 (h, $J = 4.3$ Hz, 1H), 3.18–3.09 (m, 1H), 2.13 (pd, $J = 8.0, 7.5, 4.5$ Hz, 3H), 2.03–1.62 (m, 7H); HRMS calcd for $C_{23}H_{23}N_4OCl_2$ (M+H)⁺ 441.1249, found 441.1252.

2-Cyclohexyl-N-(4-iodophenyl)-1H-imidazo[4,5-c]quinolin-4-amine (35).—

Compound **35** was synthesized following the general procedure E described above using **46h** (10 mg, 0.035 mmol) and **47b** (38.0 mg, 0.17 mmol). The crude was purified by silica gel column (10–20% ethyl acetate/hexane) to afford 10.0 mg (61%) of a white solid (HPLC $t_R = 16.7$ min): ¹H NMR (400 MHz, chloroform-*d*) δ 7.97 (d, $J = 8.3$ Hz, 1H), 7.90 (d, $J = 8.4$ Hz, 2H), 7.80–7.62 (m, 3H), 7.54 (t, $J = 7.8$ Hz, 1H), 7.36 (t, $J = 7.6$ Hz, 1H), 3.06–2.94 (m, 1H), 2.22 (d, $J = 12.8$ Hz, 2H), 1.95 (d, $J = 12.8$ Hz, 2H), 1.82 (d, $J = 13.0$ Hz, 1H), 1.69 (q, $J = 12.2$ Hz, 2H), 1.56–1.31 (m, 3H); HRMS calcd for $C_{22}H_{22}N_4I$ (M+H)⁺ 469.0889, found 469.0898.

2-Cyclohexyl-N-(4-bromophenyl)-1H-imidazo[4,5-c]quinolin-4-amine (36).—

Compound **36** was synthesized following the general procedure E described above using **46h** (15.0 mg, 0.052 mmol) and **47c** (49.0 mg, 0.28 mmol). The crude was purified by silica gel column (10–20% ethyl acetate/hexane) to afford 2.0 mg (10%) of a white solid (HPLC $t_R = 15.7$ min): $^1\text{H NMR}$ (400 MHz, chloroform-*d*) δ 7.98 (t, $J = 9.4$ Hz, 2H), 7.81–7.68 (m, 2H), 7.58–7.51 (m, 1H), 7.46 (d, $J = 2.0$ Hz, 1H), 7.36 (t, $J = 7.5$ Hz, 1H), 3.00 (tt, $J = 11.9$, 3.6 Hz, 1H), 2.26–2.17 (m, 2H), 1.94 (dt, $J = 12.3$, 3.8 Hz, 2H), 1.82 (d, $J = 13.1$ Hz, 1H), 1.69 (qd, $J = 12.3$, 3.4 Hz, 2H), 1.55–1.31 (m, 4H); HRMS calcd for $\text{C}_{22}\text{H}_{22}\text{N}_4\text{Br}$ (M+H) $^+$ 421.1028, found 421.1029.

Synthesis of 37 from a Heck Reaction Using 36.**Methyl (E)-3-(4-((2-cyclohexyl-1H-imidazo[4,5-c]quinolin-4-**

yl)amino)phenyl)acrylate (37).—2-Cyclohexyl-*N*-(4-bromophenyl)-1*H*-imidazo[4,5-*c*]quinolin-4-amine **36** (15.0 mg, 0.036 mmol), methyl acrylate (9 μL , 0.10 mmol, 1 equiv), palladium acetate (1.0 mg, 4.4 μmol , 2.8 equiv), and triethylamine (15 μL , 0.11 mmol, 3 equiv) were added successively to 2 mL of DMF in a 50 mL sealed tube. The reaction mixture was purged with $\text{N}_2(\text{g})$ at rt for 30 min and then stirred at 140 °C for 24 h. The product was diluted with ethyl acetate (5 mL) and filtered through a short silica plug. The filtrate was concentrated by rotary evaporator and then co-evaporated with toluene (2×2 mL) to obtain a crude residue, which was purified by flash chromatography using a 0.75–1.0% methanol in dichloromethane solvent system to afford 2.8 mg (18%) of compound **37** as a white solid (*E*-isomer, HPLC purity: 98%; $t_R = 13.3$ min): $^1\text{H NMR}$ (400 MHz, CDCl_3) δ 9.74 (s, 1H), 8.12 (s, 2H), 8.00 (d, $J = 8.4$ Hz, 1H), 7.82 (s, 1H), 7.70 (d, $J = 15.9$ Hz, 1H), 7.55 (dd, $J = 8.0$, 5.9 Hz, 3H), 7.37 (t, $J = 7.5$ Hz, 1H), 6.37 (d, $J = 15.9$ Hz, 1H), 3.81 (s, 3H), 2.99 (d, $J = 17.2$ Hz, 1H), 2.22 (d, $J = 12.8$ Hz, 2H), 1.94 (d, $J = 12.9$ Hz, 3H), 1.88–1.74 (m, 1H), 1.69 (td, $J = 12.4$, 3.3 Hz, 2H), 1.48 (q, $J = 12.6$ Hz, 2H). HRMS calcd for $\text{C}_{26}\text{H}_{27}\text{N}_4\text{O}_2$ (M+H) $^+$ 427.2134, found 427.2133.

Synthesis of 38 by a Sonogashira Reaction of 35.**2-Cyclohexyl-N-(4-((5-chlorothiophen-2-yl)ethynyl)phenyl)-1H-imidazo[4,5-c]quinolin-4-amine (38).—**

2-Chloro-5-ethynylthiophene (141 mg, 1.06 mmol, 5.0 equiv), 2-cyclohexyl-*N*-(4-iodophenyl)-1*H*-imidazo[4,5-*c*]quinolin-4-amine **35** (100 mg, 0.214 mmol, 1.0 equiv), bis(triphenylphosphine) palladium(II) dichloride (30.0 mg, 42.8 μmol , 5 mol%), copper(I) iodide (4.0 mg, 21.4 μmol , 2.5 mol%), and triethylamine (298 μL , 2.14 mmol, 10 equiv) were added successively to 4 mL of dry DMF in a round-bottom flask. The reaction mixture was purged with $\text{N}_2(\text{g})$ at rt for 30 min and then stirred at 80 °C for 4 h under $\text{N}_2(\text{g})$. The reaction mixture was cooled to the rt, diluted with ethyl acetate (10 mL), and filtered through a silica plug. The filtrate was concentrated by rotary evaporator and then co-evaporated with toluene (2×3 mL) to obtain a crude residue, which was purified by flash chromatography using a 15% ethyl acetate in hexane eluent system to provide 10 mg (10%) of compound **38** as a white solid (HPLC purity: 96%; $t_R = 16.3$ min): $^1\text{H NMR}$ (400 MHz, chloroform-*d*) δ 8.07 (d, $J = 7.5$ Hz, 2H), 8.00 (d, $J = 8.3$ Hz, 1H), 7.79 (d, $J = 7.1$ Hz, 1H), 7.57–7.45 (m, 3H), 7.35 (s, 1H), 7.02 (d, $J = 3.9$ Hz, 1H), 6.81 (d, $J = 3.9$ Hz, 1H), 2.97 (tt, $J = 11.8$, 3.6 Hz, 1H), 2.19 (d, $J = 11.8$

Hz, 2H), 1.92 (d, $J = 13.0$ Hz, 2H), 1.80 (d, $J = 12.7$ Hz, 1H), 1.68 (d, $J = 12.2$ Hz, 2H), 1.45 (d, $J = 12.7$ Hz, 4H); HRMS calcd for $C_{28}H_{24}N_4SCl$ (M+H)⁺ 483.1410, found 483.1412.

2-(Heptan-4-yl)-N-(4-iodophenyl)-1H-imidazo[4,5-c]quinolin-4-amine (39).—

Compound **39** was synthesized following the general procedure E described above using **46h** (195 mg, 0.64 mmol) and **47b** (424 mg, 1.94 mmol). The crude was purified by silica gel column (10–20% ethyl acetate/hexane) to afford 33 mg (11%) of a white solid (HPLC $t_R = 18.6$ min): ¹H NMR (400 MHz, chloroform-*d*) δ 8.14–7.98 (m, 1H), 7.88 (d, $J = 8.4$ Hz, 1H), 7.67 (t, $J = 7.4$ Hz, 2H), 7.59–7.46 (m, 3H), 7.32 (t, $J = 7.5$ Hz, 1H), 3.05 (tt, $J = 9.0$, 5.7 Hz, 1H), 1.90–1.67 (m, 4H), 1.34–1.15 (m, 4H), 0.86 (t, $J = 7.3$ Hz, 6H). HRMS calcd for $C_{23}H_{26}N_4I$ (M+H)⁺ 485.1202, found 485.1200.

6-Step Synthesis Protocol for 1H-imidazo-[4,5-c]quinolin-4-amine Derivatives.

3-Nitroquinoline-2,4-diol (41).¹⁹—According to the literature procedure,¹⁹ quinoline-2,4-diol (2.0 g, 12.41 mmol) was added to 12 mL of concentrated nitric acid in a 50 mL round-bottom flask. The reaction mixture was stirred for 10 min at rt and heated in an oil bath at 75 °C for 15 min. The reaction mixture was cooled to rt and poured on a crushed ice–water mixture to obtain a precipitate. The suspension was filtered, and the solid was washed with cold water and dried to obtain 2.43 g (95%) product as a nitrate salt (yellow solid).

2,4-Dichloro-3-nitroquinoline (42).¹⁹—The nitrate salt of 3-nitroquinoline-2,4-diol (**41**, 2.0 g, 9.7 mmol) was added to 17 mL of phenylphosphonic dichloride in a 50 mL round-bottom flask. The flask was fitted with a condenser and stirred the reaction mixture in an oil bath at 135 °C for 3 h. The reaction mixture was cooled to rt, poured slowly on a crushed ice–water mixture, and stirred vigorously to obtain the light brown clay-like precipitate. The mixture was filtered using a fritted funnel, and the precipitate was washed with cold water and dried under air to afford 2.05 g (87%) of crude product as an orange solid.

2-Chloro-3-nitroquinolin-4-amine (43).¹⁹—2,4-Dichloro-3-nitroquinoline (**42**, 2.0 g, 8.0 mmol) and 25% aq. ammonia (6 mL, 80 mmol, 10 equiv) were added to 20 mL of acetonitrile in a 100 mL glass pressure vessel. The mixture was stirred at 50 °C for 6 to 7 h. The reaction mixture was diluted with water (20 mL) and extracted with a mixture of ethyl acetate and methanol (95:5, 2 × 50 mL). The organic layer was separated, dried over MgSO₄, filtered, and concentrated by rotary evaporation to obtain 1.7 g (97%) of crude product as a yellow solid.

2-Chloroquinoline-3,4-diamine (44).¹⁹—To a 100 mL sealed vessel, 2-chloro-3-nitroquinolin-4-amine (**43**, 2.0 g, 9.0 mmol, 1.0 equiv), 30 mL of EtOH: H₂O (4:1), 4 N hydrochloric acid (~10 mL) and Fe powder (2.5 g, 45 mmol, 5 equiv) were added, and the reaction mixture was stirred at 75 °C for 3 h. The reaction mixture was cooled to rt and filtered through a short silica plug, and the plug was washed with EtOH:H₂O (95:5, 20 mL). The combined filtrate was neutralized with aq. NaOH/KOH until pH ~7.0. The product was extracted with a mixture of ethyl acetate and methanol (95:5, 2 × 100 mL). The organic layer was separated, dried over MgSO₄, filtered, and concentrated by rotary evaporation,

leaving a residue. The residue was purified by silica chromatography with 2% methanol in dichloromethane as an eluent to obtain 1.2 g (70%) product as a brown solid.

Synthesis of Commercially Unavailable Carboxylic Acids (45c,l,m,t).

5,5,5-Trifluoro-2-(3,3,3-trifluoropropyl)-pentanoic Acid (45c).—³² In a 50 mL round-bottom flask equipped with a stir bar were added ethyl 2-cyanoacetate (0.91 mL, 8.54 mmol, 1.0 equiv, Scheme S2), 3-bromo-1,1,1-trifluoropropane (2.0 mL, 18.8 mmol, 2.2 equiv), potassium carbonate (2.48 g, 17.9 mmol, 2.1 equiv) and 21 mL of DMF (~0.4 M). The reaction mixture was flushed with nitrogen and stirred at 60 °C for 48 h. The reaction mixture was cooled to rt, and the solvent was removed under reduced pressure by rotary evaporation to obtain a crude residue as a mixture of ethyl 2-cyano-5,5,5-trifluoropentanoate and ethyl 2-cyano-5,5,5-trifluoro-2-(3,3,3-trifluoropropyl)pentanoate **57**. The residue (1.37 g, 4.49 mmol, 1.0 equiv) was dissolved in aq. NaOH (21 mL, ~9.0 g, 225 mmol, 50 equiv), and tetrabutylammonium bromide (303 mg, ~21 mol%) was added to the flask. The reaction mixture was stirred under reflux at 90 °C for 36 h. 1 M aq. HCl was added to the reaction mixture until pH ~7. The mixture was extracted with ethyl acetate, and the organic layer was washed with water. The organic layer was dried over MgSO₄, filtered, and solvent evaporated in vacuo to provide the product as a black-brown oil, which was distilled under high vacuum at 170–180 °C to afford 300 mg (16%) crude product, assuming purity of ~50% (by ¹⁹F and ¹H NMR): ¹⁹F NMR (chloroform-*d*) δ -66.65; ¹H NMR (400 MHz, chloroform-*d*) δ 10.91–10.86 (m, 1H), 3.06–2.98 (m, 1H), 2.46 (ddt, *J* = 14.1, 9.6, 5.4 Hz, 1H), 2.27–2.01 (m, 3H), 1.97–1.83 (m, 2H), 1.75 (ddt, *J* = 13.7, 10.8, 5.5 Hz, 2H), 1.68–1.55 (m, 1H), 1.45–1.29 (m, 1H), 0.94 (td, *J* = 7.4, 1.2 Hz, 2H).

General Method for Favorskii Rearrangement^{59,60} to Prepare 45l,m.

The appropriate cyclic ketone (1.25 mmol, 1.0 equiv, Scheme S3), *N*-bromosuccinimide (1.40 mmol, 1.0–1.1 equiv) and *p*-toluenesulfonic acid (0.13 mmol, 10 mol%)⁶¹ were added to 5 mL of dichloromethane in a 15 mL round-bottom flask. The reaction mixture was stirred at rt for 16 h. The solvent was removed under reduced pressure by rotary evaporation to obtain a residue. The residue was dissolved in 10% ethyl acetate in hexane and then passed through a short silica plug. The filtrate was concentrated by rotary evaporation to obtain the α -brominated cyclic ketone as an oily residue, which was used for the next step without further purification.

In a 25 mL round-bottom flask, the crude α -brominated cyclic ketone **59a,b** (0.43 mmol) and sodium methoxide (232 mg, 4.3 mmol) were dissolved in 8 mL of methanol. The reaction mixture was stirred overnight and then refluxed for 30 min. 1 M aq. HCl was added to the reaction mixture until pH ~7. The reaction mixture was diluted with water (10 mL) and extracted with ethyl acetate (2 \times 20 mL). The organic layer was separated, dried over MgSO₄, filtered, and concentrated by rotary evaporation to get a crude product. Purification by silica gel chromatography using a 20% ethyl acetate in hexane eluent system to provide white solid products.

Cyclononancarboxylic acid (45l).—Compound **45l** was synthesized following the Favorskii rearrangement procedure described above using **58a** (100 mg, 0.65 mmol). The

crude was purified by silica gel column (20% ethyl acetate in hexane) to afford 79 mg (27%) of a white solid: $^1\text{H NMR}$ (400 MHz, $\text{DMSO-}d_6$) δ 11.97 (s, 1H), 2.38 (ddq, J = 12.7, 8.6, 4.5 Hz, 1H), 1.74 (d, J = 4.0 Hz, 2H), 1.44 (d, J = 7.0 Hz, 14H). Alternatively, a solution of crude α -brominated cyclic ketone (**59a**, 145 mg, 0.622 mmol, 1.0 eq.) in 3 mL of 10% aq. KOH (10 eq.) was refluxed for 3 h. The reaction mixture was cooled to the room temperature and was acidified with dil. HCl until the pH ~ 5–6. The reaction mixture was diluted with EtOAc (20 mL), and separated the layers. The aqueous phase was washed with EtOAc (2 \times 10 mL), and the combined EtOAc layer was dried over Na_2SO_4 and filtered. The filtrate was concentrated by rotary evaporation to obtain the crude material, which was purified by silica column to obtain a colorless oil. Yield: 410 mg (76%).

Cyclodecanecarboxylic acid (45m).—Compound **45m** was synthesized following the Favorskii rearrangement procedure described above using **58b** (50 mg, 0.30 mmol). The crude was purified by silica gel column (20% ethyl acetate in hexane) to afford 89 mg (29%) of a white solid: $^1\text{H NMR}$ (400 MHz, $\text{DMSO-}d_6$) δ 12.01 (s, 1H), 2.57 (d, J = 6.4 Hz, 1H), 1.82–1.45 (m, 18H).

Synthesis of **45t** by a Diels–Alder Reaction and a Subsequent Hydrolysis Reaction.

((1*R*,2*R*,4*R*)- and (1*S*,2*S*,4*S*)-bicyclo[2.2.2]oct-5-ene carboxylic acid (**45t**). Toluene (2 mL) was added to a 15 mL glass pressure tube containing 1,3-cyclohexadiene **60** (0.50 mL, 5.2 mmol, 1.0 equiv, Scheme S4) and methyl acrylate (0.52 mL, 5.78 mmol, 1.1 equiv). The solution was purged with $\text{N}_2(\text{g})$ and then sealed. The reaction mixture was stirred at 180 °C for 20 h. The reaction mixture was cooled to rt, and the solvent evaporated by rotary evaporation to afford the mixture of *endo* and *exo* isomers as a clear oil. The racemic *endo* product (carboxylate methyl ester) was isolated as a clear oil (402 mg, 49% yield) by silica gel chromatography using 5% ethyl acetate in hexane as the eluent system.

The *endo* carboxylate methyl ester (80.0 mg, 0.48 mmol) was dissolved in 5 mL of methanol in a 25 mL round-bottom flask, and an aq. NaOH solution (1.5 M, 5 mL) was added. The reaction mixture was stirred at rt for 1 h. 1 M aq. HCl was added to the reaction mixture until pH ~ 7. The reaction mixture was diluted with water (10 mL) and extracted with ethyl acetate (2 \times 20 mL). The organic layer was separated, dried over MgSO_4 , filtered, and concentrated by rotary evaporation to obtain the desired 400 mg (54%) of the carboxylic acid **45t**: $^1\text{H NMR}$ (400 MHz, $\text{DMSO-}d_6$) δ 11.91 (s, 1H), 6.25 (s, 1H), 6.10 (s, 1H), 2.85 (d, J = 3.4 Hz, 1H), 2.53 (d, J = 7.4 Hz, 2H), 1.65 (s, 1H), 1.60–1.48 (m, 2H), 1.48–1.39 (m, 1H), 1.16 (ddd, J = 13.4, 8.9, 3.5 Hz, 2H).

General Procedures for 2-Substituted-4-chloro-1*H*-imidazo[4,5-*c*]quinolines (**46b,c,e,h,j-t**).

Procedure A.—2.0 g PPA (per 50 mg of 2-chloroquinoline-3,4-diamine) was weighed in a 5 mL round-bottom flask. 2-Chloroquinoline-3,4-diamine (1.0 equiv) and the appropriate carboxylic acid **45c,e,h,k-n** (1.2 equiv) were added to the flask. The reaction mixture was stirred at 120 °C for 5 h. The reaction mixture was quenched by pouring on a crushed ice–water mixture. The ice–water mixture was neutralized with aq. K_2CO_3 (2 M) until pH 8–9 under stirring. The reaction mixture was extracted with ethyl acetate and then washed with water and brine several times. The organic layer was dried over MgSO_4 , filtered, and

removed the solvent by rotary evaporation to obtain the crude product, purified by silica column to obtain the 1*H*-imidazo[4,5-*c*]quinoline derivative with 15–25% ethyl acetate in hexane as the eluent system.

Procedure B.—The appropriate carboxylic acid **45b,j,o–t** (1.4 equiv) and NMI (3.5 equiv), were added to 4 mL acetonitrile in a 15 mL round-bottom flask with stirring, followed by 2-chloroquinoline-3,4-diamine (1 equiv) and TCFH (1.5 equiv). The reaction mixture was stirred at 60 °C for 5 h. The cooled reaction mixture was diluted with ethyl acetate, and the organic layer was washed with brine (3×). The organic layer was dried over MgSO₄ and filtered, transferred to a 50 mL round-bottom flask, and the solvent evaporated by a rotary evaporator. A 1:1 solution of aq. NaOH (15 equiv of NaOH in 10 mL of H₂O):methanol (10 mL) was added with stirring. The reaction mixture was refluxed at 90 °C for 3 h. The cooled reaction mixture was diluted with ethyl acetate, and the organic layer was washed with brine (3 × 10 mL) followed by water (3 × 10 mL). The organic layer was dried over MgSO₄, evaporated in vacuo, and the resulting residue was used in the final reaction step without further purification.

General Stannylation Procedure to Prepare **48** and **49** from **39**.

2-(Heptan-4-yl)-*N*-(4-iodophenyl)-1*H*-imidazo-[4,5-*c*]quinolin-4-amine **39** (0.10 mmol, 1.0 equiv), bis(triphenylphosphine)palladium(II) dichloride (20 μmol, 20 mol%), and hexamethylditin or hexabutyliditin (0.5 mmol, 5.0 equiv) were added to 2 mL of 1,4-dioxane in a 10 mL round-bottom flask. The reaction mixture was purged with N₂(g) at rt for 30 min and stirred at 70 °C for 2.5 h or until the starting material disappeared (monitored by TLC). The reaction mixture was cooled to the rt, diluted with ethyl acetate (10 mL), and filtered through a short silica plug. The filtrate was concentrated by rotary evaporator and then co-evaporated with toluene (2 × 3 mL) to obtain a crude residue, purified by flash chromatography using a 10% ethyl acetate in hexane eluent system.

2-(Heptan-4-yl)-N-(4-(trimethylstannyl)phenyl)-1H-imidazo[4,5-c]quinolin-4-amine (48).

Compound **48** was synthesized following the stannylation procedure described above using **39** (49.0 mg, 0.10 mmol) and hexamethylditin (105 μL, 0.50 mmol). The crude was purified by silica gel column (20% ethyl acetate in hexane) to afford 5.0 mg (10%) of a white solid: ¹H NMR (400 MHz, chloroform-*d*) δ 8.04 (s, 2H), 7.83 (s, 1H), 7.57–7.47 (m, 3H), 7.40–7.28 (m, 2H), 3.11–2.95 (m, 1H), 1.87–1.70 (m, 4H), 1.40–1.28 (m, 4H), 0.89 (d, *J* = 7.3 Hz, 6H), 0.39–0.17 (m, 9H); HRMS calcd for C₂₆H₃₅N₄Sn (M+H)⁺ 523.1884, found 523.1882.

2-(Heptan-4-yl)-N-(4-(tributylstannyl)phenyl)-1H-imidazo[4,5-c]quinolin-4-amine (49).

Compound **49** was synthesized following the stannylation procedure described above using **39** (50.0 mg, 0.10 mmol) and hexabutyliditin (300 μL, 0.50 mmol). The crude was purified by silica gel column (20% ethyl acetate in hexane) to afford 9.0 mg (13%) of a white solid: ¹H NMR (400 MHz, chloroform-*d*) δ 8.05 (d, *J* = 8.8 Hz, 1H), 7.97 (s, 1H), 7.79 (d, *J* = 21.8 Hz, 2H), 7.57–7.44 (m, 2H), 7.38 (t, *J* = 7.7 Hz, 1H), 7.32 (s, 1H), 3.04 (s, 1H), 1.80 (dq, *J* = 12.3, 7.1, 6.3 Hz, 4H), 1.65

(tt, $J = 8.2, 6.5$ Hz, 6H), 1.56 (ddt, $J = 10.4, 8.0, 3.7$ Hz, 4H), 1.38–1.28 (m, 19H), 0.91 (dd, $J = 8.9, 7.3$ Hz, 18H); HRMS calcd for $C_{35}H_{53}N_4Sn$ (M+H)⁺ 649.3292, found 649.3293.

Pharmacological Methods.

Cell Culture.—HEK-293 cell lines expressing wild-type human, mouse, or chimeric A₃AR were cultured and maintained in Dulbecco's modified eagle medium (DMEM) along with 10% fetal bovine serum, 1% penicillin/streptomycin, and 0.6 mg/mL G418.

Membrane Preparation.—HEK-293 cells stably expressing wild-type human, mouse, or chimeric A₃ARs were washed in phosphate-buffered saline followed by homogenization in hypotonic lysis buffer containing 10 mM Na⁺-HEPES, 10 mM EDTA, and 1 mM benzamidine (pH 7.4) and then centrifuged at 27000*g* for 30 min at 4 °C. Cell pellets were subsequently resuspended in He buffer containing 10 mM Na⁺-HEPES, 1 mM EDTA, and 1 mM benzamidine (pH 7.4) and re-centrifuged. Supernatant was discarded and remaining pellets were resuspended in He buffer containing 10% sucrose and stored at –20 °C.

Single-Point Dissociation Study.—~0.3 nM of [¹²⁵I]50 was incubated with 50 μg of HEK-293 cell membranes expressing A₃ARs for 2 h at rt in 100 μL of binding buffer (50 mM Tris-HCl [pH 7.4], 10 mM MgCl₂, 1 mM EDTA, and 1 unit/mL adenosine deaminase). The assay was started by adding 100 μM of the nonselective agonist 51, along with 10 μM of the PAM or vehicle (DMSO). After 60 min, the bound [¹²⁵I]50 was measured following rapid filtration using GF/C filters. Data are expressed as the amount of radioligand left remaining after 60 min as a percent of the vehicle. A gamma counter measured [¹²⁵I]50-bound receptors in the filters. Nonspecific binding was determined for all assays by incubation of membranes in the presence of 100 μM 51. All experiments were performed in technical and biological triplicate. Raw CPM values for agonist and modulator tubes and control tubes were used to calculate statistical significance using a two-tailed paired Student's *t* test.

Single-Point Equilibrium Binding Study.—HEK-293 membranes (50 μg) were incubated at rt with ~0.3 nM [¹²⁵I]50 and 10 μM modulator of vehicle (DMSO) for 18 h in 100 μL of binding buffer (50 mM Tris-HCl [pH 7.4], 10 mM MgCl₂, 1 mM EDTA and 1 unit/mL adenosine deaminase). At that point, the amount of radioligand was measured by rapid filtration using GF/C filters. Data are expressed as the amount of specific binding as a % change from vehicle. Nonspecific binding was determined for all assays by incubation in the presence of 100 μM 51. All experiments were performed in technical and biological triplicate. Binding data of agonists influenced by modulators were statistically compared to the control using a two-tailed unpaired Student's *t* test.

GTP-γS Binding Method for Measuring Receptor Activation.—[³⁵S]GTP-γS binding assays were conducted to assess the direct effects of modulators on receptor activation. Five μg membranes overexpressing the indicated A₃AR were pretreated with modulators for 1 h in 100 μL GTP-γS binding buffer (50 mM Tris-HCl [pH 7.4], 10 mM MgCl₂, 1 mM EGTA, 100 mM NaCl, 0.004% CHAPS, and 0.5% BSA). To block endogenously expressed A_{2B}ARs found in HEK-293 cells, AR antagonists 62 and 63 were

added, with each at a final concentration of each of 300 nM. 1 Unit/mL of ADA was added to break down any endogenous adenosine that might have been present. Reactions were initiated by the addition of ~0.2 nM [³⁵S]GTP γ S and agonist in 100 μ L GTP γ S binding buffer and incubated for 2 h. Reactions were stopped with membranes being harvested by rapid filtration through Whatman GF/B filters presoaked for 2 h in GTP γ S binding buffer containing an additional 0.02% CHAPS using a cell harvester (Brandel, Gaithersburg, MD). Radioactivity trapped in the filters was measured by liquid scintillation counting. Nonspecific binding of [³⁵S]GTP γ S was measured in the presence of 10 μ M unlabeled GTP γ S. Agonist potency and maximal efficacy at 0.1 μ M, 1.0 μ M, and 10 μ M were statistically compared to the control using one-way ANOVA with multiple comparisons and Bonferroni post hoc test.

ADMET Methods.

Both in vitro and in vivo ADMET properties were determined by JRF India of JRF Global (Gujarat, India).

In Vivo Assays.⁴⁷—The animal breeding facility, Jai Research Foundation, provided healthy adult male rats (*Rattus norvegicus*) of Wistar strain (RccHan:WIST). Rats were 6 to 10 weeks old at the start of acclimation. The weight variation of rats was \pm 20% of mean body weight (b.wt.) at the start of acclimation. Table S6 shows the experimental outline for the *in vivo* study of pharmacokinetics using rats.

Two routes of administration, intravenous and oral, were used to determine A₃AR PAM bioavailability. The dose level for the G₁ intravenous route was 0.5 mg/kg b.wt., and the dose levels for the G₂₋₄ oral route were 1, 3, and 10 mg/kg b.wt. The A₃AR PAM-DMSO solution was diluted with an aq. solution of 20% 2-hydroxypropyl- β -cyclodextrin (HPBCD) for the intravenous administration, creating a final volume ratio of DMSO to HPBCD, 10:90. An equal volume of Kolliphor EL (polyoxyl castor oil) was added to the A₃AR PAM-DMSO solution for oral administration, followed by phosphate buffer saline (PBS). The final volume ratio of DMSO:Kolliphor:PBS for the oral administration was 15:15:70.

200 μ L blood was collected from the jugular vein from each rat group on the day of dosing at 0.083, 0.25, 0.5, 1, 2, 4, 8, 12, and 24 h post dosing to assess the A₃AR PAM PK profile through intravenous administration. Blood samples were collected in prelabeled microcentrifuge tubes with the anticoagulant heparin (20 IU/mL of blood). After collection, samples were inverted 4 to 5 times, placed on ice, and centrifuged at 9000 rpm for 10 min. Plasma was frozen at -70 °C.

Pharmacokinetic analysis of the frozen plasma concentration–time data was performed using the non-compartmental model of the WinNonlin software. Estimated parameters were the maximum plasma concentration (C_{max}), the time to achieve peak plasma concentration (T_{max}), the area under the plasma concentration–time curve until the last measured time point (AUC_{0-last}), the area under the plasma concentration–time curve extrapolated to infinity ($AUC_{0-\infty}$), the terminal elimination half-life ($T_{1/2}$), the mean residence time (MRT), volume of distribution (V_d), the elimination rate constant (k_{el}), the bioavailability (%*F*), and the clearance (Cl).

In Vitro Assays.—Plasma stability was measured in three species: human, rat, and mouse at 0 to 120 min by liquid chromatography mass spectroscopy–mass spectroscopy (LCMS-MS). % A₃AR PAM remaining was provided at 120 min and $t_{1/2}$ (min). The methods were as described.⁴⁷

HepG2 cytotoxicity was measured using the CellTiter-Glo Luminescent Cell Viability assay. This assay determined the number of live cells in culture by measuring the ATP metabolism of active cells. 10 to 40 K cells were placed in a 96-well plate. The A₃AR PAMs were incubated with live cells for 48 h. Eight dilutions were made with varying concentrations of A₃AR PAM ranging from 30 μ M to 0.2 μ M and incubated. Verapamil/Rifampicin were used as a reference compound. Analysis was done via luminometry. Data was reported as an IC₅₀ value, the concentration of A₃AR PAM that reduces cell viability by 50% (ATP measurement).

Human Ether-à-go-go Related Gene (hERG) potassium channels are involved in cardiac action potential re-polarization. hERG assay measures the % inhibition of the potassium channels by the A₃AR PAM. The assay used HEK-293 cells stably transfected with the hERG potassium channel. A₃AR PAM concentrations were prepared using serial half-log dilutions, starting at 30 μ M. A₃AR PAMs were incubated with the hERG-expressing cells for 2 h. A₃AR PAMs bound to the hERG ion channel were identified by their ability to displace the tracer (Predictor hERG Tracer Red), which resulted in a lower fluorescence polarization using a TAMRA fluorescent polarization filter. E-4031 is a reference compound. % inhibition was reported as the ratio of half-maximum inhibitory concentration of the hERG channel (hERG IC₅₀, μ M) to the peak serum concentration of unbound drug (C_{max}).

CYP inhibition was determined with a cocktail approach. A₃AR PAMs at six concentrations in duplicate (30 μ M to 0.12 μ M) were incubated with liver microsomes (human, rat, mice) containing the CYP panel with known substrates (1A2, phenacetin (10 μ M); 2C9, diclofenac (5 μ M); 2C19, omeprazole (5 μ M); 2D6, dextromethorphan (5 μ M); 3A4, midazolam (2 μ M)), 1 mM of NADPH cofactor, 1 μ M miconazole (pan inhibitor) in plasma. Analysis of substrates was done by LC-MS/MS. This approach reported A₃AR PAM concentrations which produced 50% inhibition of CYPs (IC₅₀ value, μ M). LCMS-MS quantified metabolites by area ratio: acetaminophen (1A2), 4-OH-diclofenac (2C9), 5-OH-omeprazole (2C19), dextromethorphan (2D6), and 1-OH-midazolam (3A4).

Microsomal stability assays were done using human, rat, and mouse liver microsomes containing the following enzymes: CYPs, flavin monooxygenases, carboxylesterases, and epoxide hydrolase. A₃AR PAMs were in 3 μ M concentrations duplicates and mixed with 1 mM NADPH and 0.5 g/mL of human, rat, or mouse liver microsomes. Samples were taken from five time periods (0.5, 15, 30, 60, 90, 120 min) and analyzed by LC-MS/MS. The average half-life (min) and % remaining at 120 min was reported.

Caco-2 cell permeability assay measured the rate of transport of a compound across the Caco-2 cell line (21-day process consisting of bidirectional monitoring of absorptive (A-B) and secretory (B-A) fluxes). The Caco-2 cell line originated from a human colon carcinoma,

having a polarized monolayer, an apical surface, and intercellular junctions. The cells were exposed to the A₃AR PAM (10 μM) in an HBSS buffer with 2% BSA. Samples were gathered at 0- and 120 min. Samples were analyzed by LCMS-MS. Positive controls were atenolol, digoxin, and propranolol. Apparent permeability (P_{app} – 10⁶ cm/sec), efflux ratio, and % recovery were reported.

pION solubility of each A₃AR PAM at pH 7.4 was measured using the pION buffer method. Each A₃AR PAM was added to the pION buffer in sufficient amount to reach 500 μM (hypothetically). Sampling was done at 18 h. Positive controls were albendazole and flurbiprofen. Solubility was reported for each A₃AR PAM as mean solubility (μg/mL).

Plasma protein binding was determined and expressed as the % unbound A₃AR PAM in the plasma of three species (rat, mouse, and human). Cellulose membranes in potassium phosphate buffer (100 mM, pH 7.4) were exposed to 10 μM of A₃AR PAM and 500 μL of plasma. Samples were loaded into dialysis cells and maintained in an incubator at 37 °C at 100 rpm. Samples were collected into prelabeled microfuge tubes at 0 and 5 h. The samples were vortexed and centrifuged. Supernatants were analyzed by LC-MS/MS. % binding reported: 1–40% low bound, 41–70% medium bound, 71–100% highly bound.

Simulated gastrointestinal fluids were used to determine whether A₃AR PAMs are chemically stable in the stomach at low pH 1–2 or in the intestine pH 6–8. Five μM of each A₃AR PAM was added to simulated gastric fluid (SGF) and simulated intestinal fluid (SIF). Sampling was done at 0- and 120 min time points. Method of analysis was LC-MS/MS by area ratio. % A₃AR PAM at 120 min was reported.

Prediction of Log *D*, TPSA, and BBB log([brain]:[blood]) was performed using the StarDrop software (v. 7.2), <https://www.optibrium.com/stardrop-installers/>.⁴⁵

Molecular Docking.

Maestro (Maestro 2021–2) of the Schrödinger (New York, NY, USA) suite was used for basic molecular modeling operations. Ligands were drawn and minimized with OPLS4⁶² force field with water solution model. The model of hA₃AR was generated in a previous work,⁴⁹ using an antagonist-bound hA₁AR X-ray structure as a template and a refinement with Induced Fit Docking of the antagonist **64**. The following tautomeric states were employed for histidines: protonation at N_δ nitrogen for H272^{7.43} (HSD according to the CHARMM nomenclature) and at the N_ε nitrogen for H793.21, H953.37, H1244.39, H158EL2, and H3048.65. The Ballesteros–Weinstein sequence-based numbering scheme⁶³ is indicated as superscript for all residues throughout the text.

Compounds **17** and **7** were docked to the receptor structure using the IFD tool of the Schrödinger suite.^{50,65} An inner box of 10 Å box and outer box of 30 Å, centered on the barycenter of residues F168^{EL2} and N250^{6.55}, were employed. Residues within 3 Å of the ligand (with the addition of Q167^{EL2} and V169^{EL2}) were optimized, and the XP scoring function⁶⁷ was used for the refinement stage. A maximum of 20 poses was generated for each ligand, and the 5 top scoring ones (according to the IFDScore) were minimized with

Prime MM-GBSA tool, using implicit membrane, VSGB solvation model, OPLS4 force field, and minimizing residues within 3 Å from the ligand.

The Semiempirical Extended Tight-Binding Program Package, XTB,⁶⁴ was used for the dihedral scan. The geometry of the common *N*-(3,4-dichlorophenyl)-1*H*-imidazo[4,5-*c*]quinolin-4-amine scaffold was optimized with the GFN2-XTB method, and then a relaxed dihedral scan of the torsional angle defined by atoms N5–C4–N(amino)–Cp(phenyl) was performed from 0° to 360° in 72 steps (freezing the scanned dihedral with a force constant of 50 E_h/a₀²).

Supplementary Material

Refer to Web version on PubMed Central for supplementary material.

ACKNOWLEDGMENTS

We acknowledge support from the NIH Intramural Research Program (NIDDK, ZIADK031117), the NIH Extramural Research Program (NHLBI, R01 grant HL133589), and the MCW Therapeutic Accelerator Program. We thank John Lloyd (NIDDK) for mass spectral determinations and Robert O'Connor (NIDDK) for NMR spectra and Joel Linden (Univ. of Virginia) for providing ABOPX for iodination. We thank Dilip K. Tosh, Young-Hwan Jung, Zhiwei Wen, and Kiran S. Toti (NIDDK) for chemical advice. We thank Dr. Bryan L. Roth (Univ. North Carolina at Chapel Hill) and National Institute of Mental Health's Psychoactive Drug Screening Program (Contract No. HHSN-271-2008-00025-C) for screening data.

ABBREVIATIONS USED

ADA	adenosine deaminase
AR	adenosine receptor
DAT	dopamine transporter
DIPEA	diisopropylethylamine
DPFGSE	Double Pulsed Field Gradient Selective Echo
HBSS	Hanks's balanced salt solution
HEK-293	human embryonic kidney 293
HMA	hexamethylene amiloride
HPBCD	2-hydroxypropyl- β -cyclodextrin
IFD	induced fit docking
KOR	κ opioid receptor
MOR	μ opioid receptor
NAM	negative allosteric modulator
NMI	<i>N</i> -methylimidazole
PAM	positive allosteric modulator

PDSP	NIMH Psychoactive Drug Screening Program
POPC	1-palmitoyl-2-oleoyl- <i>sn</i> -glycero-3-phosphocholine
PPA	polyphosphoric acid
RMSF	root-mean-square-fluctuation
TCFH	tetramethylchloroformamidinium hexafluorophosphate
TPSA	topological polar surface area
TSPO	translocator protein

REFERENCES

- (1). Gessi S; Merighi S; Varani K Adenosine receptors: The status of the art. In *The Adenosine Receptors*; Borea PA., Varani K., Gessi S., Merighi S., Vincenzi F., Eds.; Springer International Publishing, 2018; pp 1–11.
- (2). Linden J Adenosine in tissue protection and tissue regeneration. *Mol. Pharmacol.* 2005, 67 (5), 1385. [PubMed: 15703375]
- (3). Borea PA; Varani K; Vincenzi F; Baraldi PG; Tabrizi MA; Merighi S; Gessi S The A₃ adenosine receptor: History and perspectives. *Pharmacol. Rev.* 2015, 67 (1), 74. [PubMed: 25387804]
- (4). Jacobson KA; Tosh DK; Jain S; Gao Z-G Historical and current adenosine receptor agonists in preclinical and clinical development. *Front. Cell. Neurosci.* 2019, 13, 124. [PubMed: 30983976]
- (5). Changeux J-P; Edelstein SJ Allosteric mechanisms of signal transduction. *Science* 2005, 308 (5727), 1424–1428. [PubMed: 15933191]
- (6). Draper-Joyce CJ; Bhola R; Wang J; Bhattarai A; Nguyen ATN; Cowie-Kent I; O’Sullivan K; Chia LY; Venugopal H; Valant C; Thal DM; Wootten D; Panel N; Carlsson J; Christie MJ; White PJ; Scammells P; May LT; Sexton PM; Danev R; Miao Y; Glukhova A; Imlach WL; Christopoulos A Positive allosteric mechanisms of adenosine A₁ receptor-mediated analgesia. *Nature* 2021, 597 (7877), 571–576. [PubMed: 34497422]
- (7). Conn PJ; Christopoulos A; Lindsley CW Allosteric modulators of GPCRs: a novel approach for the treatment of CNS disorders. *Nat. Rev. Drug. Discovery* 2009, 8 (1), 41–54. [PubMed: 19116626]
- (8). Merighi S; Simioni C; Lane R; IJzerman AP Regulation of second messenger systems and intracellular pathways. In *A3 Adenosine Receptors from Cell Biology to Pharmacology and Therapeutics*; Borea PA., Ed.; Springer Netherlands, 2010; pp 61–73.
- (9). Foster DJ; Conn PJ Allosteric modulation of GPCRs: New insights and potential utility for treatment of schizophrenia and other CNS disorders. *Neuron* 2017, 94 (3), 431–446. [PubMed: 28472649]
- (10). Schaddelee MP; Read KD; Cleypool CG; IJzerman AP; Danhof M; de Boer AG Brain penetration of synthetic adenosine A₁ receptor agonists in situ: role of the rENT1 nucleoside transporter and binding to blood constituents. *Eur. J. Pharm. Sci.* 2005, 24 (1), 59–66. [PubMed: 15626578]
- (11). Liston TE; Hinz S; Müller CE.; Holstein DM.; Wendling J; Melton RJ; Campbell M; Korinek WS; Suresh RR; Sethre-Hofstad DA; Gao ZG; Tosh DK; Jacobson KA; Lechleiter JD Nucleotide P2Y₁ receptor agonists are in vitro and in vivo prodrugs of A1/A3 adenosine receptor agonists: implications for roles of P2Y1 and A1/A3 receptors in physiology and pathology. *Purinergic Signal* 2020, 16 (4), 543–559. [PubMed: 33129204]
- (12). Fredholm BB; IJzerman AP; Jacobson KA; Linden J; Müller, C. E. International Union of Basic and Clinical Pharmacology. LXXXI. Nomenclature and classification of adenosine receptors—an update. *Pharmacol. Rev.* 2011, 63 (1), 1–34. [PubMed: 21303899]
- (13). Liston TE; Hama A; Boltze J; Poe RB; Natsume T; Hayashi I; Takamatsu H; Korinek WS; Lechleiter JD Adenosine A1R/A3R (adenosine A1 and A3 receptor) Agonist AST-004 reduces

- brain infarction in a nonhuman primate model of stroke. *Stroke* 2022, 53 (1), 238–248. [PubMed: 34802248]
- (14). Jacobson KA; Gao Z-G Allosteric modulators of adenosine, P2Y and P2X receptors. *Allosterism in Drug Discovery; The Royal Society of Chemistry, 2017; Chapter 11, pp 247–270.*
- (15). Slosky LM; Caron MG; Barak LS Biased allosteric modulators: New frontiers in GPCR drug discovery. *Trends Pharmacol. Sci.* 2021, 42 (4), 283–299. [PubMed: 33581873]
- (16). Gao Z-G; Melman N; Erdmann A; Kim SG; Müller CE.; IJzerman AP.; Jacobson KA. Differential allosteric modulation by amiloride analogues of agonist and antagonist binding at A₁ and A₃ adenosine receptors. *Biochem. Pharmacol.* 2003, 65 (4), 525–534. [PubMed: 12566079]
- (17). Gao Z-G; Van Muijlwijk-Koezen JE; Chen A; Müller CE.; IJzerman AP.; Jacobson KA. Allosteric modulation of A₃ adenosine receptors by a series of 3-(2-pyridinyl)isoquinoline derivatives. *Mol. Pharmacol.* 2001, 60 (5), 1057. [PubMed: 11641434]
- (18). Gao Z-G; Kim SG; Soltysiak KA; Melman N; IJzerman AP; Jacobson KA Selective allosteric enhancement of agonist binding and function at human A₃ adenosine receptors by a series of imidazoquinoline derivatives. *Mol. Pharmacol.* 2002, 62 (1), 81–89. [PubMed: 12065758]
- (19). Göblyös A; Gao Z-G; Brussee J; Connestari R; Santiago SN; Ye K; IJzerman AP; Jacobson KA Structure–activity relationships of new 1H-imidazo[4,5-c]quinolin-4-amine derivatives as allosteric enhancers of the A₃ adenosine receptor. *J. Med. Chem.* 2006, 49 (11), 3354–3361. [PubMed: 16722654]
- (20). Kim Y; de Castro S; Gao Z-G; IJzerman AP; Jacobson KA Novel 2- and 4-substituted 1H-imidazo[4,5-c]quinolin-4-amine derivatives as allosteric modulators of the A₃ adenosine receptor. *J. Med. Chem.* 2009, 52 (7), 2098–2108. [PubMed: 19284749]
- (21). Heitman LH; Göblyös A; Zweemer AM; Bakker R; Mulder-Krieger T; van Veldhoven JPD; de Vries H; Brussee J; IJzerman AP A series of 2,4-disubstituted quinolines as a new class of allosteric enhancers of the adenosine A₃ receptor. *J. Med. Chem.* 2009, 52 (4), 926–931. [PubMed: 19161279]
- (22). Gao Z-G; Verzijl D; Zweemer A; Ye K; Göblyös A; IJzerman AP; Jacobson KA Functionally biased modulation of A₃ adenosine receptor agonist efficacy and potency by imidazoquinolinamine allosteric enhancers. *Biochem. Pharmacol.* 2011, 82 (6), 658–668. [PubMed: 21718691]
- (23). Itzhak I; Cohen S; Fishman S; Fishman P A₃ adenosine receptor allosteric modulator CF602 reverses erectile dysfunction in a diabetic rat model. *Andrologia* 2022, 54, No. e14498. [PubMed: 35732294]
- (24). Fisher CL; Fallot LB; Wan TC; Keyes RF; Suresh RR; Rothwell AC; Gao Z-G; McCorvy JD; Smith BC; Jacobson KA; Auchampach JA Structure activity relationship of dual action purine nucleoside allosteric modulators of the A₃ adenosine receptor. *ACS Pharmacol. Transl. Sci.* 2022, 5 (8), 625–641. [PubMed: 35983277]
- (25). Gao D; Xiao Q; Zhang M; Li Y Design, synthesis and biological evaluation of benzyloxyphenyl-methylaminophenol derivatives as STAT3 signaling pathway inhibitors. *Bioorg. Med. Chem.* 2016, 24 (11), 2549–2558.
- (26). Beutner GL; Young IS; Davies ML; Hickey MR; Park H; Stevens JM; Ye Q TCFH–NMI: Direct access to N-acyl imidazoliums for challenging amide bond formations. *Org. Lett.* 2018, 20 (14), 4218–4222. [PubMed: 29956545]
- (27). Ruiz-Castillo P; Buchwald SL Applications of palladium-catalyzed C–N cross-coupling reactions. *Chem. Rev.* 2016, 116 (19), 12564–12649. [PubMed: 27689804]
- (28). Ghodke PP; Pradeepkumar PI Nucleoside modification using Buchwald-Hartwig amination reactions. In *Palladium-Catalyzed Modification of Nucleosides, Nucleotides and Oligonucleotides*; Kapdi AR., Maiti D., Sanghvi YS., Eds.; Elsevier, 2018; Chapter 10, pp 295–333.
- (29). Fors BP; Krattiger P; Strieter E; Buchwald SL Water-mediated catalyst preactivation: An efficient protocol for C–N cross-coupling reactions. *Org. Lett.* 2008, 10 (16), 3505–3508. [PubMed: 18620415]
- (30). Meanwell NA Fluorine and fluorinated motifs in the design and application of bioisosteres for drug design. *J. Med. Chem.* 2018, 61 (14), 5822–5880. [PubMed: 29400967]

- (31). Miller MA; Sletten EM A general approach to biocompatible branched fluorinated tags for increased solubility in perfluorocarbon solvents. *Org. Lett.* 2018, 20 (21), 6850–6854. [PubMed: 30354161]
- (32). Kouji Y; Mikiro Y Novel fluorine-containing compound, its preparation and antiepileptic agent. Patent JPH0421652A, Jan 24, 1992.
- (33). Denmark SE; Edwards JP A comparison of (chloromethyl)- and (iodomethyl)zinc cyclopropanation reagents. *J. Org. Chem.* 1991, 56 (25), 6974–6981.
- (34). Singh V; Tosh DK; Mobin SM Synthesis of embellished bicyclo[2.2.2]octenones and a sigmatropic 1,2-acyl shift in an excited state: a novel and stereoselective route to (±)-hirsutic acid C and complicatic acid. *Tetrahedron Lett.* 2004, 45 (8), 1729–1732.
- (35). Singh V; Pal S; Tosh DK; Mobin SM Molecular complexity from aromatics. Cycloaddition of cyclohexa-2,4-dienones, sigmatropic 1,2-acyl shift and ring-closing metathesis: a new, efficient, and stereoselective synthesis of (±)-hirsutic acid C and medium ring carbocycles. *Tetrahedron* 2007, 63 (11), 2446–2454.
- (36). Appendino G; Spagliardi P; Sterner O; Milligan S Structure–activity relationships of the estrogenic sesquiterpene ester ferutinin. modification of the terpenoid core. *J. Nat. Prod.* 2004, 67 (9), 1557–1564. [PubMed: 15387659]
- (37). Dikošová L; Laceková J; Záborský O; Fischer R Synthesis of 3-substituted isoxazolidin-4-ols using hydroboration–oxidation reactions of 4,5-unsubstituted 2,3-dihydroisoxazoles. *Beilstein J. Org. Chem.* 2020, 16, 1313–1319. [PubMed: 32595779]
- (38). Beghetto V; Scrivanti A; Bertoldini M; Aversa M; Zancanaro A; Matteoli U A Practical, enantioselective synthesis of the fragrances canthoxal and silvial[®], and evaluation of their olfactory activity. *Synthesis* 2015, 47 (02), 272–288.
- (39). Qadir M; Möchel T; Hii KK Examination of ligand effects in the Heck arylation reaction. *Tetrahedron* 2000, 56 (40), 7975–7979.
- (40). Thorand S; Krause N Improved procedures for the palladium-catalyzed coupling of terminal alkynes with aryl bromides (Sonogashira coupling). *J. Org. Chem.* 1998, 63 (23), 8551–8553.
- (41). Sonogashira K Development of Pd–Cu catalyzed cross-coupling of terminal acetylenes with sp²-carbon halides. *J. Organomet. Chem.* 2002, 653 (1), 46–49.
- (42). Sloan NL; Luthra SK; McRobbie G; Pimlott SL; Sutherland A A one-pot radioiodination of aryl amines via stable diazonium salts: preparation of ¹²⁵I-imaging agents. *Chem. Commun.* 2017, 53 (80), 11008–11011.
- (43). Auchampach JA; Gizewski E; Wan TC; de Castro S; Brown GG; Jacobson KA Synthesis and pharmacological characterization of [¹²⁵I]MRS5127, a high affinity, selective agonist radioligand for the A₃ adenosine receptor. *Biochem. Pharmacol.* 2010, 79, 967–973. [PubMed: 19917269]
- (44). Du L; Gao Z-G; Paoletta S; Wan TC; Gizewski ET; Barbour S; van Veldhoven JPD; IJzerman AP; Jacobson KA; Auchampach JA Species differences and mechanism of action of A₃ adenosine receptor allosteric modulators. *Purinergic Signalling* 2018, 14, 59–71. [PubMed: 29170977]
- (45). Segall MD Multi-parameter optimization: Identifying high quality compounds with a balance of properties. *Curr. Pharm. Des.* 2012, 18, 1292–1310. [PubMed: 22316157]
- (46). Besnard J; Ruda GF; Setola V; Abecassis K; Rodriguiz RM; Huang X-P; Norval S; Sassano MF; Shin AI; Webster LA; Simeons FR; Stojanovski L; Prat A; Seidah NG; Constam DB; Bickerton GR; Read KD; Wetsel WC; Gilbert IH; Roth BL; Hopkins AL Automated design of ligands to polypharmacological profiles. *Nature* 2012, 492 (7428), 215–220. [PubMed: 23235874]
- (47). Tosh DK; Salmaso V; Campbell RG; Rao H; Bitant A; Pottie E; Stove CP; Liu N; Gavrilova O; Gao ZG; Auchampach JA; Jacobson KA A₃ adenosine receptor agonists containing dopamine moieties for enhanced interspecies affinity. *Eur. J. Med. Chem.* 2022, 228, 113983. [PubMed: 34844790]
- (48). Larregieu CA; Benet LZ Drug discovery and regulatory considerations for improving in silico and in vitro predictions that use Caco-2 as a surrogate for human intestinal permeability measurements. *AAPS J.* 2013, 15 (2), 483–497. [PubMed: 23344793]

- (49). Suresh RR; Gao ZG; Salmaso V; Chen E; Campbell RG; Poe RB; Liston TE; Jacobson KA Selective A₃ adenosine receptor antagonist radioligand for human and rodent species. *ACS Med. Chem. Lett.* 2022, 13 (4), 623–631. [PubMed: 35450351]
- (50). Sherman W; Day T; Jacobson MP; Friesner RA; Farid R Novel procedure for modeling ligand/receptor induced fit effects. *J. Med. Chem.* 2006, 49, 534–553. [PubMed: 16420040]
- (51). Genheden S; Ryde U The MM/PBSA and MM/GBSA methods to estimate ligand-binding affinities. *Expert Opin. Drug Discovery* 2015, 10, 449–461.
- (52). Jacobson KA; Gao ZG; Göblyös A; IJzerman AP Allosteric modulators of purine and pyrimidine receptors. *Adv. Pharmacol.* 2011, 61, 187–220. [PubMed: 21586360]
- (53). Ciancetta A; Jacobson KA Structural probing and molecular modeling of the A₃ adenosine receptor: A focus on agonist binding. *Molecules* 2017, 22 (3), 449. [PubMed: 28287473]
- (54). Gao ZG; Ye K; Göblyös A; IJzerman AP; Jacobson KA Flexible modulation of agonist efficacy at the human A₃ adenosine receptor by an imidazoquinoline allosteric enhancer LUF6000 and its analogues. *BMC Pharmacol* 2008, 8, 20. [PubMed: 19077268]
- (55). van Galen PJM; Nissen P; van Wijngaarden I; IJzerman AP; Soudijn W 1H-imidazo[4,5-c]quinolin-4-amines: novel non-xanthine adenosine antagonists. *J. Med. Chem.* 1991, 34, 1202–1206. [PubMed: 2002461]
- (56). Schön MP; Schön M; Klotz K-N The small antitumoral immune response modifier imiquimod interacts with adenosine receptor signaling in a TLR7- and TLR8-independent fashion. *J. Invest. Dermatol.* 2006, 126 (6), 1338–1347. [PubMed: 16575388]
- (57). Christopoulos A; Changeux JP; Catterall WA; Fabbro D; Burris TP; Cidlowski JA; Olsen RW; Peters JA; Neubig RR; Pin JP; Sexton PM; Kenakin TP; Ehlert FJ; Spedding M; Langmead CJ International Union of Basic and Clinical Pharmacology. XC. Multisite pharmacology: recommendations for the nomenclature of receptor allosterism and allosteric ligands. *Pharmacol. Rev.* 2014, 66 (4), 918–947. [PubMed: 25026896]
- (58). Sato J; Makita N; Iiri T Inverse agonism: the classic concept of GPCRs revisited. *Endocr. J.* 2016, 63 (6), 507–514. [PubMed: 26961122]
- (59). Kende AS The Favorskii rearrangement of haloketones. *Org. Reactions* 2011, 261–316.
- (60). Tsuchida N; Yamazaki S; Yamabe S A new mechanism for the Favorskii rearrangement. *Org. Biomol. Chem.* 2008, 6 (17), 3109–3117. [PubMed: 18698470]
- (61). Sekhar T; Thriveni P; Venkateswarlu A; Daveedu T; Peddanna K; Sainath SB One-pot synthesis of thiazolo[3,2-a]pyrimidine derivatives, their cytotoxic evaluation and molecular docking studies. *Spectrochim. Acta Part A: Mol. Biomol. Spectr.* 2020, 231, 118056.
- (62). Lu C; Wu C; Ghoreishi D; Chen W; Wang L; Damm W; Ross GA; Dahlgren MK; Russell E; Von Bargen CD; Abel R; Friesner RA; Harder ED OPLS4: improving force field accuracy on challenging regimes of chemical space. *J. Chem. Theory Comput.* 2021, 17, 4291–4300. [PubMed: 34096718]
- (63). Ballesteros JA; Weinstein H [19] Integrated methods for the construction of three-dimensional models and computational probing of structure-function relations in G protein-coupled receptors. *Methods Neurosci* 1995, 25, 366–428.
- (64). Bannwarth C; Ehlert S; Grimme S GFN2-xTB-an accurate and broadly parametrized self-consistent tight-binding quantum chemical method with multipole electrostatics and density-dependent dispersion contributions. *J. Chem. Theory Comput.* 2019, 15, 1652–1671. [PubMed: 30741547]
- (65). Miller EB; Murphy RB; Sindhikara D; Borrelli KW; Grisewood MJ; Ranalli F; Dixon SL; Jerome S; Boyles NA; Day T; Ghanakota P; Mondal S; Rafi SB; Troast DM; Abel R; Friesner RA Reliable and accurate solution to the induced fit docking problem for protein–ligand binding. *J. Chem. Theory. Comput.* 2021, 17 (4), 2630–2639. [PubMed: 33779166]
- (66). Kooistra AJ; Mordalski S; Pándy-Szekeres G; Esguerra M; Mamyrbekov A; Munk C; Keser , G. M.; Gloriam, D. E. GPCRdb in 2021: integrating GPCR sequence, structure and function. *Nucleic Acids Res.* 2021, 49, D335–D343. [PubMed: 33270898]
- (67). Friesner RA; Murphy RB; Repasky MP; Frye LL; Greenwood JR; Halgren TA; Sanschagrin PC; Mainz DT Extra precision glide: docking and scoring incorporating a model of hydrophobic

enclosure for protein-ligand complexes. *J. Med. Chem.* 2006, 49, 6177–6196. [PubMed: 17034125]

Author Manuscript

Author Manuscript

Author Manuscript

Author Manuscript

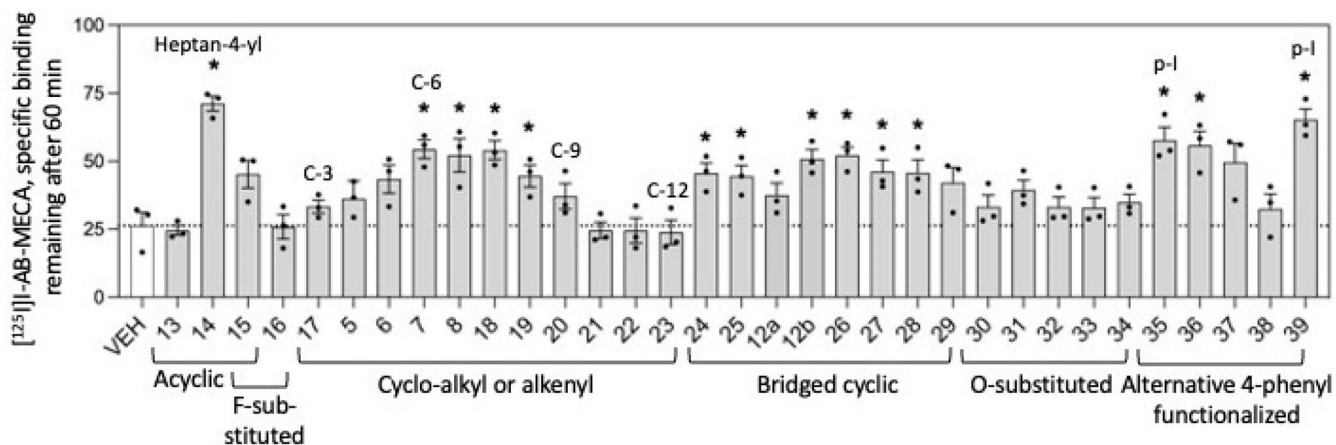


Figure 1.

Effect of 1*H*-imidazo[4,5-*c*]quinolin-4-amine derivatives on the dissociation of [¹²⁵I]**50** using hA₃ARs. HEK-293 membranes stably overexpressing the hA₃AR were incubated with ~0.3 nM [¹²⁵I]**50** and 10 μM of the indicated modulator for 3 h. The addition of 100 μM **51** initiated dissociation. The amount of radioligand left remaining after 60 min was measured. Statistical significance was calculated by a two-tailed Student's *t* test (*n* = 3; * denotes *P* < 0.05). Data are presented as mean ± SEM.

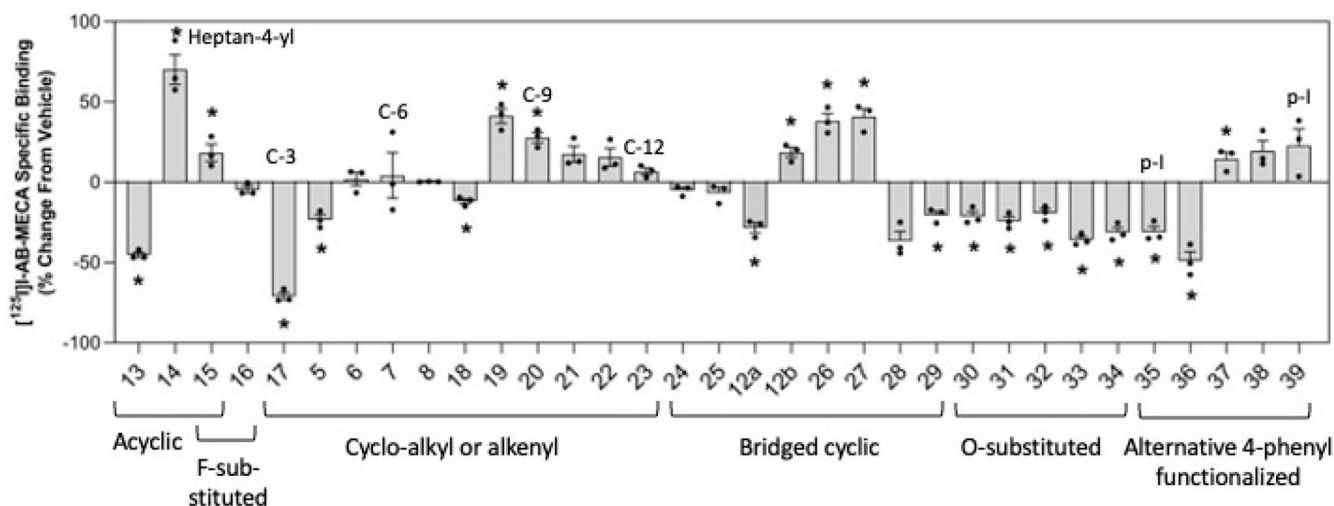
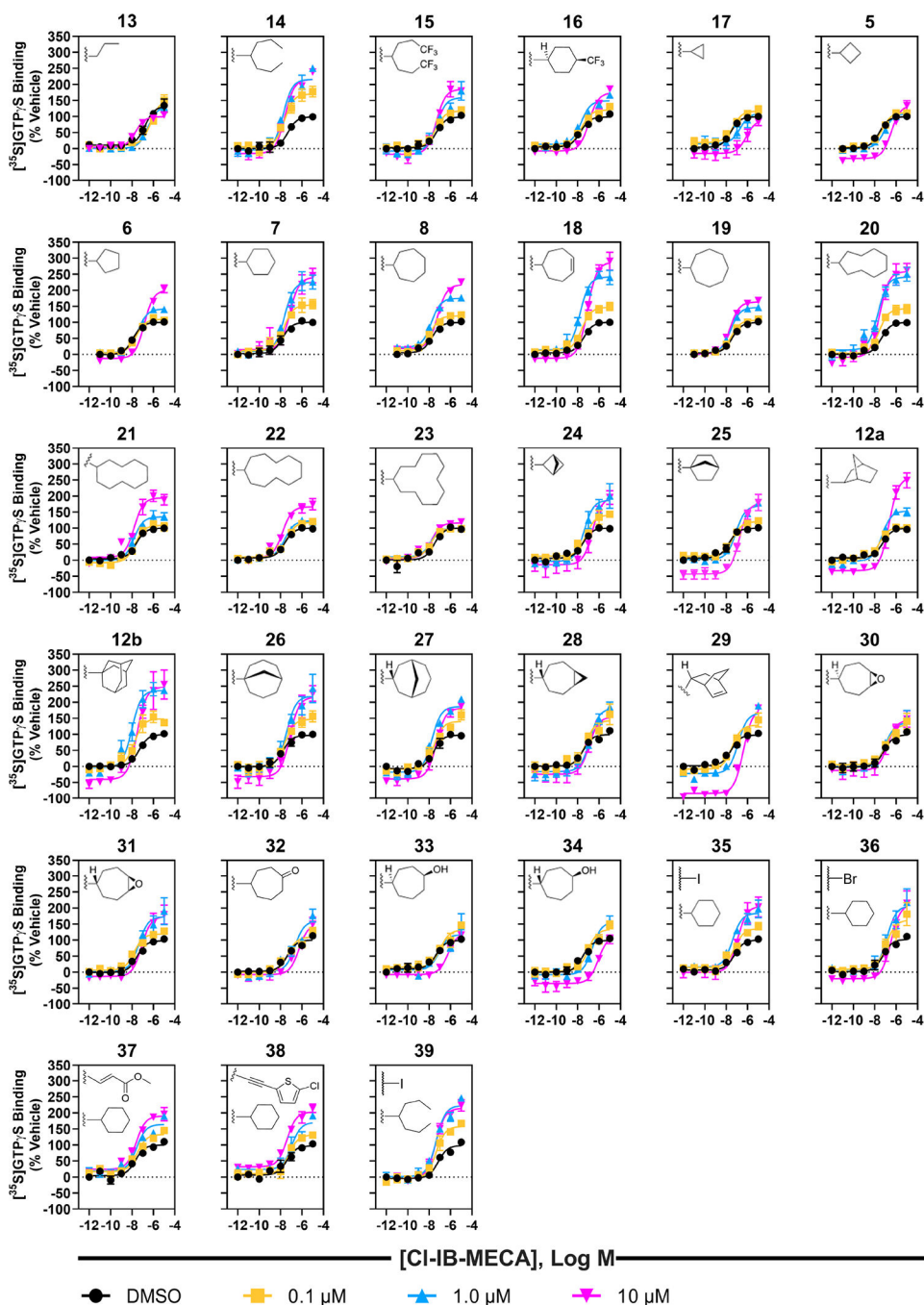


Figure 2. Effect of PAM derivatives on equilibrium binding of [125 I]**50** at the hA₃AR. HEK-293 cell membranes stably overexpressing the hA₃AR were incubated with ~ 0.3 [125 I]**50** and $10 \mu\text{M}$ of the indicated modulator for ~ 18 h to reach equilibrium. The amount of specific binding was determined, and % change from the vehicle was calculated. Statistical significance was determined by two-tailed paired Student's *t* test of raw counts per min values for modulator compared to vehicle ($n = 3$; * denotes $P < 0.05$). Data are presented as mean \pm SEM.

**Figure 3.**

Effect of 2-alkyl- and 2-cycloalkyl-substituted PAM derivatives (**5–8**, **13–23**), bridged PAM derivatives (**12a**, **12b**, **24–29**), PAM derivatives bearing hydrophilic substituents (**30–34**), and *p*-phenylamino-substituted PAM derivatives (**35–39**) on hA₃AR activation by **52** determined using [³⁵S]GTPγS binding (*n* = 3). HEK-293 cell membranes expressing hA₃AR were pretreated with **52** and modulators for 1 h, followed the addition of radiolabeled [³⁵S]GTPγS to initiate the reaction, and incubated for an additional 2 h at room temperature. AR antagonists 8-[4-[4-(4-chlorophenyl)piperazine]-1-

sulfonylphenyl]]-1-propylxanthine (**62**, PSB-603) and 4-[2-[7-amino-2-(2-furyl)-1,2,4-triazolo[1,5-*a*]-[1,3,5]triazin-5-yl-amino]ethyl]phenol (**63**, ZM241385) were added (0.3 μM each final concentration) to block any endogenously expressed $\text{A}_{2\text{B}}$ ARs. 1 unit/mL of adenosine deaminase (ADA) was added to degrade endogenous adenosine. The incubation was terminated by rapid filtration through a Whatman GF/B filter and membrane-bound radioactivity was measured by liquid scintillation spectrometry. Non-specific binding of [^{35}S]GTP γS was measured in the presence of 10 μM of unlabeled GTP γS . **52** potency and maximal efficacy was measured using DMSO, 0.1 μM , 1.0 μM , and 10 μM of the modulator. Results were normalized to concentration–response curve E_{max} values obtained by **52** with DMSO and expressed as % activation.

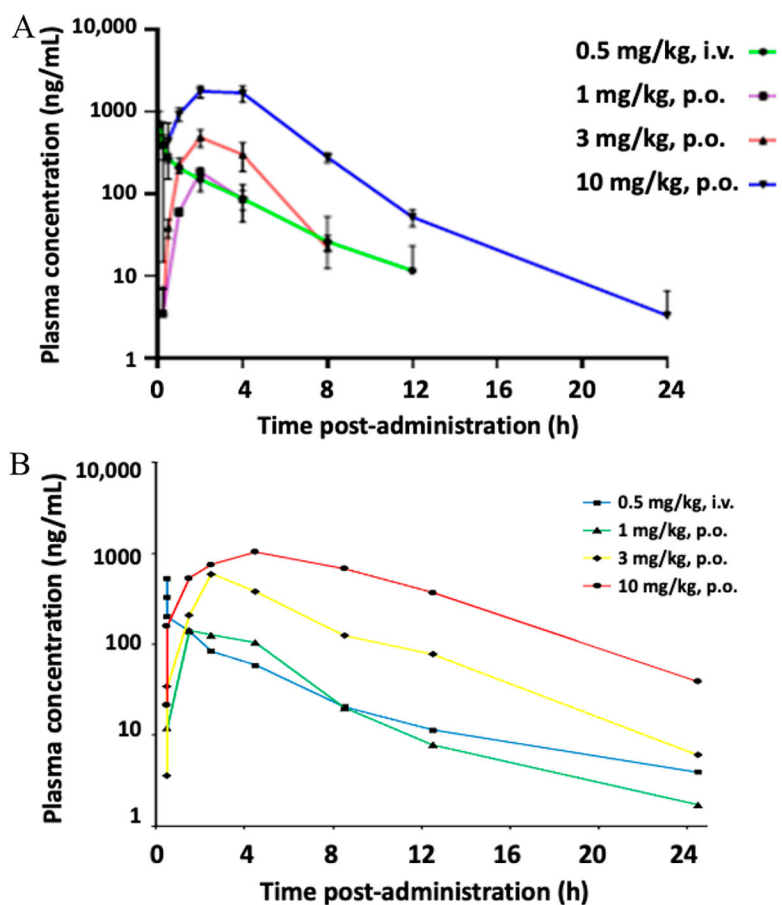


Figure 4. Mean plasma concentrations of compound **18** (A) and compound **39** (B) in Wistar rats vs multiple time points. The dose and administration route are specified above for each of the four groups (three rats in each group).

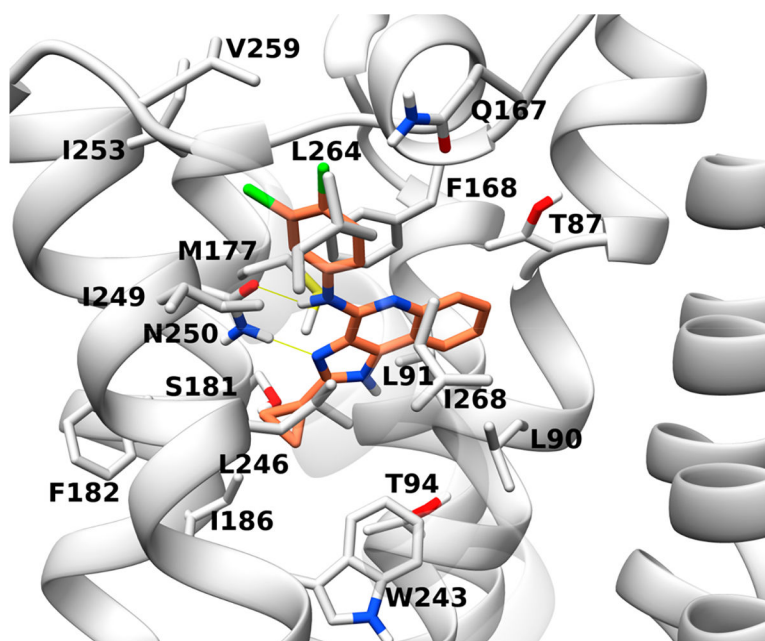
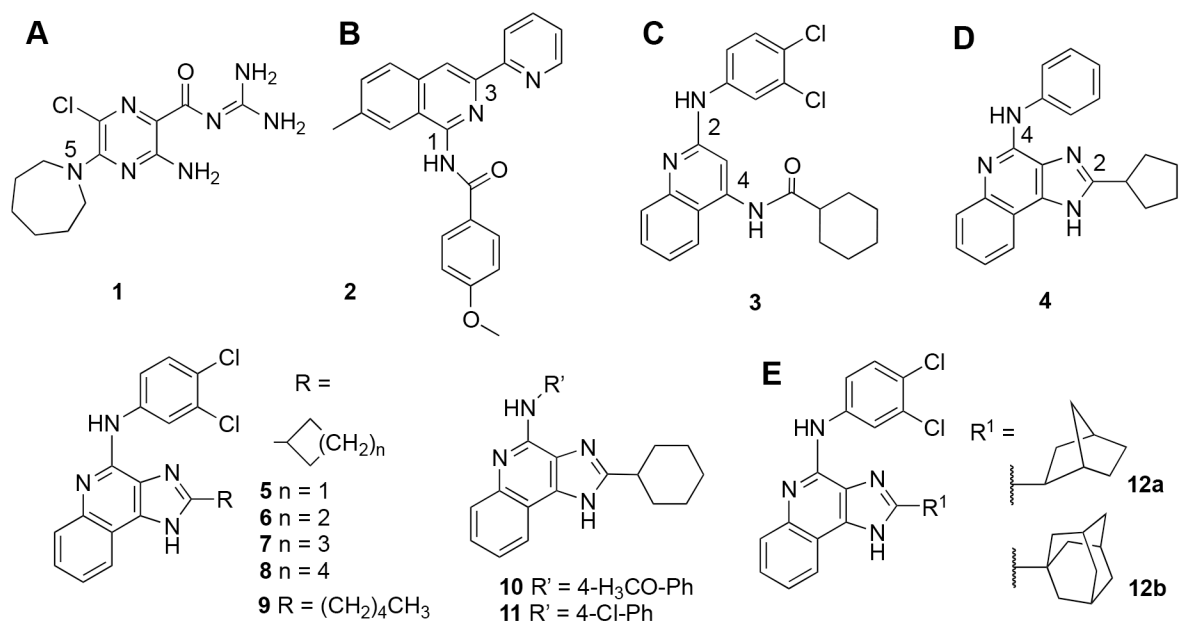
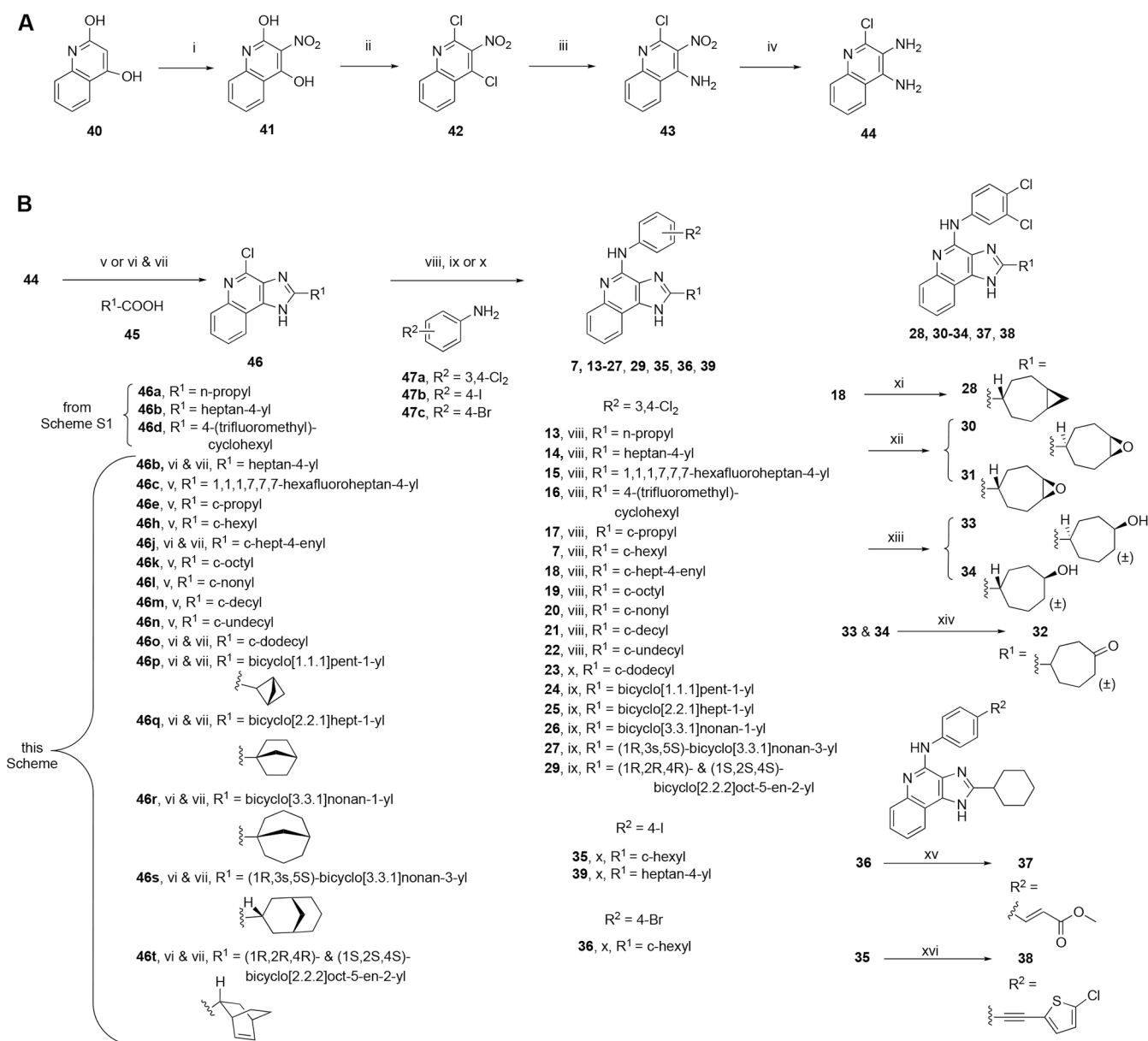


Figure 5.
Predicted favored pose of compound **17** (orange) at hA₃AR orthosteric binding site (gray).
The pose was generated through IFD followed by MM-GBSA minimization.

**Chart 1.**

(A–D) Four Classes of Heterocyclic A₃AR Allosteric Modulators [Amiloride Derivative 1 (A), 3-(2-Pyridinyl)isoquinoline 2 (B), 2,4-Disubstituted Quinoline 3 (C), and 1*H*-Imidazo[4,5-*c*]quinolin-4-amines with 2-Alkyl and 2-Cycloalkyl Substitutions (4–12) (D), Including Alternative 4-Substituted Phenylamino Derivatives and the Bulky 2-Bicycloalkyl (*exo*-Norbornanyl, 12a) and 2-Tricycloalkyl (Adamantan-1-yl, 12b) Derivatives (E)^{19,20}



Scheme 1. Six-Step Synthetic Route for 1*H*-Imidazo[4,5-*c*]quinolin-4-amine Derivatives with 2 Position and 4-Arylamino Substitutions (B), Including the Synthesis of a Common Diamino Intermediate 44 (A)^a

^aReagents and conditions: (i) HNO₃, 75 °C, 95%; (ii) PhPOCl₂, 135 °C, 87%; (iii) 28% aq. ammonia, CH₃CN, 50 °C, 97%; (iv) Fe powder, HCl, CH₃CH₂OH/H₂O, 75 °C, 70%; (v) PPA, 120 °C; (vi) TCFH, NMI, ACN, 60 °C; (vii) NaOH, H₂O:MeOH (1:1), 90 °C; (viii) Pd₂(dba)₃, tBuXPhos, *t*-BuONa, 1,4-dioxane, 100 °C, 5–51%, (ix) Pd(OAc)₂, tBuXPhos, *t*-BuONa, H₂O, 1,4-dioxane, 100 °C, 2–33%; (x) EtOH, microwave, 130 °C, 10–61%; (xi) 18, Et₂Zn, CH₂I₂, 0 °C, 13%; (xii) 18, *m*-CPBA, CHCl₃, 6–12%, 30 and 31 separated chromatographically; (xiii) 18, (CH₃)₂S·BH₃, THF, NaOH, H₂O₂, 0 °C, 8–12%, 33 and 34 separated chromatographically; (xiv) 33/34, DMP, CHCl₃, 23%; (xv) 36, Pd(OAc)₂,

$\text{CH}_2=\text{CHCOOCH}_3$, Et_3N , 140 °C, 18%; (xvi) **35**, $\text{Pd}(\text{Ph}_3\text{P})_2\text{Cl}_2$, 5-Cl-thien-2-yl-acetylene, CuI , Et_3N , 80 °C, 10%.

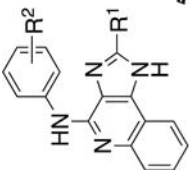



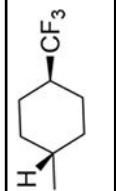

Author Manuscript

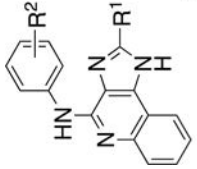
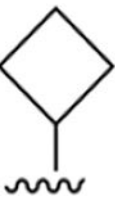

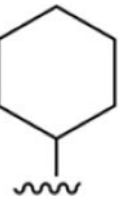
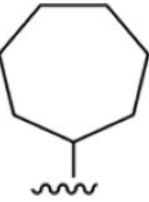
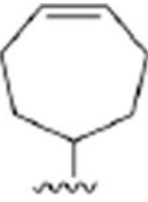
Author Manuscript

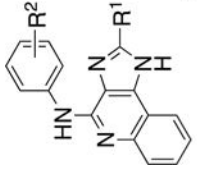
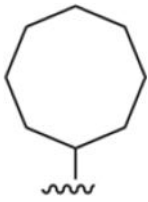


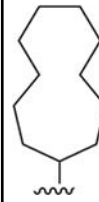
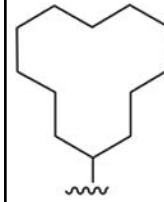
Author Manuscript

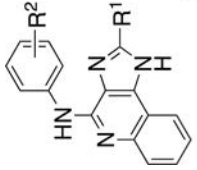

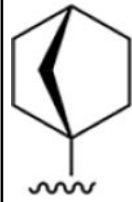

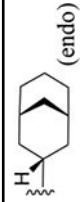

Author Manuscript

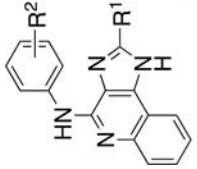

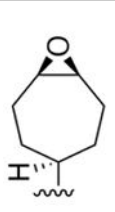
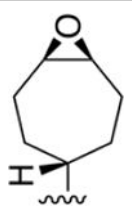
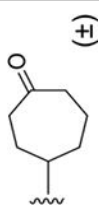
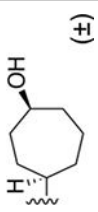
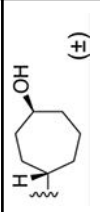
Table 1. 1*H*-Imidazo[4,5-*c*]quinolin-4-amine Derivatives Synthesized and Effects on Agonist-Induced A₃AR Activation

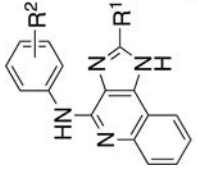
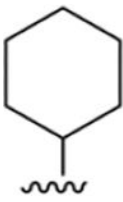
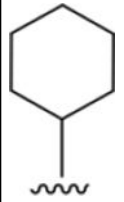
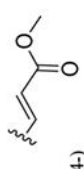
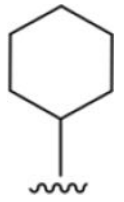
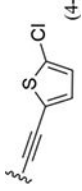
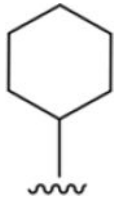


 5 – 8, 13 – 39, 48, 49		R ¹	R ²	E _{max} (%)
<i>2-alkyl and 2-cycloalkyl derivatives</i>				
13			3,4-Cl ₂	153 ± 12*
14			3,4-Cl ₂	216 ± 12*
15			3,4-Cl ₂	159 ± 13*
16			3,4-Cl ₂	150 ± 5*
17			3,4-Cl ₂	111 ± 16


 5 – 8, 13 – 39, 48, 49				
Compound	R ²	R ¹	E _{max} (°)	
5	3,4-Cl ₂		109 ± 3	
6	3,4-Cl ₂		142 ± 5*	
7	3,4-Cl ₂		225 ± 10*	
8	3,4-Cl ₂		175 ± 3*	
18	3,4-Cl ₂		241 ± 9*	

 5 – 8, 13 – 39, 48, 49		R¹	R²	Compound	E_{max} α (%)
			3,4-Cl ₂	19	146 ± 2 *
			3,4-Cl ₂	20	241 ± 12 *
			3,4-Cl ₂	21	135 ± 7 *
			3,4-Cl ₂	22	122 ± 6 *
			3,4-Cl ₂	23	101 ± 3
<i>2-bicycloalkyl derivatives</i>					

 5 – 8, 13 – 39, 48, 49				
Compound	R ²	R ¹		E _{max} α (%)
24	3,4-Cl ₂			187 ± 14 [*]
25	3,4-Cl ₂			170 ± 6 [*]
26	3,4-Cl ₂			154 ± 7 [*]
27	3,4-Cl ₂		 (endo)	237 ± 12 [*]
28	3,4-Cl ₂			219 ± 16 [*]

 5 – 8, 13 – 39, 48, 49		R¹	E_{max} α (%)
Compound	R²		
29	3,4-Cl ₂		187 ± 8 *
<i>2-cycloalkyl derivatives with hydrophilic substitution</i>			
30	3,4-Cl ₂		136 ± 11
31	3,4-Cl ₂		173 ± 14 *
32	3,4-Cl ₂	 (±)	160 ± 16 *
33	3,4-Cl ₂	 (±)	118 ± 14
34	3,4-Cl ₂	 (±)	156 ± 10 *
<i>2-alkyl and 2-cycloalkyl derivatives with modified 2-aryl/amino groups</i>			

 5 – 8, 13 – 39, 48, 49				E_{\max} α (%)
Compound	R ²	R ¹		
35	4-I		184 ± 9 *	
36	4-Br		207 ± 17 *	
37	 (4-)		164 ± 10 *	
38	 (4-)		170 ± 12 *	
39	4-I		223 ± 10 *	
48	4-Sn(CH ₃) ₃		ND	

Compound	R ²	R ¹	E _{max} a (%)
49	4-Sr((CH ₂) ₅ CH ₃) ₃		ND

5 – 8, 13 – 39, 48, 49

^aEffect of PAM derivative (1.0 μM) on [³⁵S]GTPγS binding induced by **52** using WT hA₃ARs (*n* = 3).

* *P* = 0.05 (one-way ANOVA with Bonferroni-adjusted *t* test for multiple comparisons) with respect to control in the absence of a PAM. Effects of 0.1 and 10 μM are shown in Table S4. ND, not determined.

Table 2.

Off-Target Analysis of Selected PAM Derivatives at 45 Other Receptors, Transporters, and Channels, As Determined in Radioligand Binding Assays by the PDSP^a

derivative	protein	K_i (μM)
14	5HT _{2B}	1.36
	σ_1	1.48
	σ_2	1.36
18	σ_1	4.64
	σ_2	0.575
20	σ_1	5.15
	σ_2	0.907
21	σ_2	3.62
22	D ₃	5.28
23	D ₃	7.63
	σ_1	3.02
	σ_2	2.84
26	σ_1	2.34
	σ_2	1.34
27	MOR	7.22
	σ_1	2.42
	σ_2	3.43
	KOR	5.50
	DAT	0.467
	5HT _{2B}	3.25
	35	D ₃
35	TSPO	0.427
	σ_2	3.01
	39	5HT _{2B}
39	TSPO	0.123
	σ_2	0.891

^aThese are the only hits with >50% inhibition in the primary screen at 10 μM .

Table 3.

In Vitro and In Vivo Experimental Pharmacokinetic Parameters of Compounds 18 and 39

test	reference compound(s)	compound 18	compound 39
simul. intestinal fluid % remaining at 120 min ($t_{1/2}$, min)	Verapamil 100 (>240)	100 (573)	86.2 (533)
simul. gastric fluid % remaining at 120 min $t_{1/2}$, min)	Omeprazole 0.0 (15.3)	69.1 (204)	99.7 (>240)
plasma stability % remaining at 120 min $t_{1/2}$, min, 3 species)	0.0 (0.11, h, procaine); 83.9 (414, r, diltiazem); 0.0 (0.11, m, procaine)	69.7 (159, h); 88.7 (580, r); 83.5 (695, m)	53.2 (140, h); ~100 (>240, r); ~100 (>240, m);
CYP1A2, IC ₅₀ (μM)	Miconazole, 4.55	6.99	1.31
CYP2C9, IC ₅₀ (μM)	Miconazole, 0.38	>30	32.3
CYP2C19, IC ₅₀ (μM)	Miconazole, 0.00002	>30	83.6
CYP2D6, IC ₅₀ (μM)	Miconazole, 1.64	>30	60.8
CYP3A4 (IC ₅₀ , μM)	Miconazole (0.0010)	>30	61.6
microsomal stability % remaining at 120 min ($t_{1/2}$, min, 3 species)	Testosterone 5.44 (15.6, h); 0 (1.43, r); 0 (4.33, m)	81.2 (200, h); 52.1 (70, p); 76.4 (194, m)	92.1 (>120, h); 86.3 (>120, p); 75.2 (>120, m);
plasma protein binding % bound (3 species)	Warfarin, 96.3 (h); 100 (r); 83.6 (m)	~100 (h); 99.1 (r); ~100 (m)	93.6 (h); 100 (r); 100 (m)
hERG, IC ₅₀ (μM) ^a	n/a	6.06	>30 ^b
HepG2 cell toxicity, IC ₅₀ (μM)	Verapamil, 65.2	>30	35.4
aqueous solubility pH 7.4 (μg/mL)	n/a	0.39	<0.01
oral bioavailability, $t_{1/2}$ (h) (3 mg/kg, p.o.)	n/a	28.7% F; 1.29	64.0% F; 3.44

^aFluorescence polarization hERG assay.^b27% inhibition at 30 μM.